RI-URBANS/ACTRIS GUIDANCE DOCUMMENTS ON MEASUREMENTS OF AIR QUALITY ADVANCED PARAMETERS FOR AIR QUALITY STAKEHOLDERS

ULTRAFINE PARTICLES / SIZE DISTRIBUTIONS

RI-URBANS

Research Infrastructures Services Reinforcing Air Quality Monitoring Capacities in European Urban & Industrial AreaS (GA n. 101036245)

By

IMPORTANT NOTICE

This is a preliminary version on RI-URBANS/ACTRIS guidance for this specific service tool. The final version will be produced at the end of 2024 by RI-URBANS-ACTRIS with the support for publication from AXA RESEARCH FUND. The content does not reflect the official opinion of the European Union.

23/07/2024

RI-URBANS (http://www.RIURBANS.eu) is supported by the European Commission under the Horizon 2020 – Research and Innovation Framework Programme, H2020-GD-2020, Grant Agreement number: 101036245

Authors: Meritxell García-Marlès (CSIC), Pedro Trecehera (CSIC), Xiansheng Liu (CSIC), (CNRS), Tuukka Petäjä (UHEL), Roy Harrison (UoB), Phillip Hopke (Clarckson University), Alfred Wiedensholer (TROPOS), Andrés Alastuey (CSIC) & Xavier Querol (CSIC)

RI-URBANS (http://www.RIURBANS.eu) is supported by the European Commission under the Horizon 2020 – Research and Innovation Framework Programme, H2020-GD-2020, Grant Agreement number: 101036245

Table of Contents

1. ABOUT THIS DOCUMENT 1

2. DEFINITION OF ULTRAFINE PARTICLES (UFP) AND PARTICLE NUMBER SIZE DISTRIBUTION (PNSD) 1

3. MEASUREMENT METHODS AND QUALITY CONTROL OF UFP AND PNSD 2

3.1 STATE OF HARMONISATION 2
3.1.1 CEN standards 2
3.1.2 Other relevant guidance 2
3.2 SAMPLING AND CONDITIONING 2
3.2.1 Sampling 2
3.2.2 Drying 3
3.2.3 Dilution 3
3.2.4 Performance criteria and test procedures for the sampling and conditioning system 4
3.3 DETERMINATION OF THE PNC (UFP) 4
3.3.1 Method of operation for determining PNC 4
3.3.2 CPC performance criteria and test procedures 5
3.3.3 Measurement procedure 5
3.3.4 Quality control, quality assurance and measurement uncertainty 5
3.4 DETERMINATION OF THE PNSD 5
3.4.1 Method of operation for determining PNSD with a MPSS 6
3.4.2 Correction for particle losses due to diffusion 6
3.4.3 Correction for CPC detection efficiency 6
3.4.4 MPSS performance criteria and test procedures 6
3.4.5 Measurement procedure 7
3.4.6 Quality control, quality assurance and measurement uncertainty 7
3.5 DATA MANAGEMENT 7

4. PAN-EUROPEAN OVERVIEW OF UFP AND PNSD ACROSS URBAN ENVIRONMENTS 8

4.1 INTRODUCTION 8
4.2 METHODOLOGY 9
4.2.1 UFP-PNSD Data compilation 9
4.2.2 2009-2019 trend analysis of UFP-PNSD 10
4.2.3 Determination of lung deposited surface area (LDSA) from UFP-PNSD 11
4.3 CONCENTRATIONS OF UFP AND PNSD 11
4.3.1 Particle number size distributions 12
4.3.2 Particle number concentrations 12
4.3.3 Nucleation, Aitken and Accumulation modes 13
4.3.4 Diel and seasonal patterns 14
4.3.5 2009-2019 UFP-PNSD trends 17
4.4 AMBIENT AIR PARTICULATE TOTAL LUNG DEPOSITED SURFACE AREA (LDSA) IN URBAN EUROPE 19

5. RECOMMENDATIONS AND MAIN FINDINGS 23

5.1 RECOMMENDATIONS ON MEASUREMENTS, QUALITY CONTROL AND DATA MANAGEMENT 23
5.1.1 Sampling system 23
5.1.2 Particle size range 23
5.1.3 Instrument performance 23
5.1.4 Maintenance and quality control 24
5.1.5 Calibration infrastructures 24
5.1.6 Data management 24
5.2 MAIN FINDINGS FOR PNC-PNSD IN URBAN EUROPE 24

5.2.1 Instrument and data management 24
5.2.2 Concentrations of UFP-PNSD 25
5.2.3 UFP-PNSD 2009-2019 concentration trends 25
5.2.4 Levels of aerosol Lung Deposited Surface Area (LDSA) in urban Europe 26

6. REFERENCES 26

1. ABOUT THIS DOCUMENT

This document is a connected to the Proposal for a Directive of the European Parliament and of the Council on ambient air quality and cleaner air for Europe - Mandate for negotiations with the European Parliament - Brussels, 9 November 2023. This document was prepared as part of "Research Infrastructures Services Reinforcing Air Quality Monitoring Capacities in European Urban & Industrial AreaS" (RI-URBANS) EU-project that connects the atmospheric observation expertise from Aerosols, Clouds and Trace gases Research InfraStructure, ACTRIS as well as the urban air quality observation capacities of the regulatory air quality monitoring networks.

The proposed directive underlines that the importance of emerging pollutants to air quality and well-being of the citizens. Particularly ultrafine particles (UFPs), black carbon (BC) and elemental carbon (EC), as well as ammonia (NH_3) and the oxidative potential (OP) of particulate matter (PM), need to be monitored in both rural and urban supersites in order to support scientific understanding of their effects on health and the environment, as recommended by the WHO. For Member States whose territory is less than 10,000 km^2, monitoring in supersites at urban locations would be sufficient as the levels measured could be considered as representative of the highest exposure of the population in the territory of such Member States.

To ensure that the information collected on air pollution is sufficiently representative and comparable across the Union, it is important that standardised measurement techniques and common criteria for the number and location of measuring stations are used for the assessment of ambient air quality. The aim of this document is to facilitate upscaling of measurement techniques for UFPs within air quality monitoring networks. We provide an up-to-date summary of the harmonized methodologies related to UFPs, summarize recent scientific synthesis of Pan-European observations and provide concise recommendations on the measurements of UFPs in urban environments.

This is a preliminary version on RI-URBANS/ACTRIS guidance for this specific service tool. The final version will made up RI-URBANS' deliverable D46 (D6.1, containing guidance for all service tools provided in the project) which will be produced be produced at the end of 2024 by RI-URBANS-ACTRIS, with the support for publication from AXA FOUNDATION. The content does not reflect the official opinion of the European Union.

2. DEFINITION OF ULTRAFINE PARTICLES (UFP) AND PARTICLE NUMBER SIZE DISTRIBUTION (PNSD)

As defined in the proposal for the European AQ Directive (following the WHO definition), 'ultrafine particles' (UFP) means the particles number concentrations (PNC) with a diameter less than or equal to 100 nm; UFP are measured as the PNC per cubic centimetre (cm^3) for a size range with a lower limit of 10 nm and for a size range with no restriction on the upper limit. As the number fraction of particles greater than 100nm is generally 10-30% compared to that <100nm (generally around 80%), the use of PNC without an upper limit is a good approximation to the number of UFP (<100nm).

Particle number concentration (PNC) is defined as the number of particles related to the unit volume of the carrier gas. In the new AQ Directive, PNC is used as a surrogate of UFP.

According to the CEN/TS 17434:2020, particle number size distribution (PNSD) is the frequency distribution of the particle number concentration represented as a function of the logarithm of particle size, such that the area under the distribution between two sizes is the number concentration of that size range.

3. MEASUREMENT METHODS AND QUALITY CONTROL OF UFP AND PNSD

3.1 State of harmonisation

3.1.1 CEN standards

There are two key variables regarding UFP: PNC and PNSD. Therefore, two technical specifications have been established:

Particle number concentration (PNC)

prEN16976:2023: "Ambient air - Determination of the particle number concentration of atmospheric aerosol" is currently being prepared by the Technical Committee CEN/TC 264 "Air Quality", the secretariat of which is held by DIN, and will supersede CEN/TS 16976:2016. This document describes a standard method for determining the particle number concentration in ambient air in a range up to about 10^7 cm^{-3} for averaging times equal to or larger than 1 min. The standard method is based on a Condensation Particle Counter (CPC) operated in the counting mode. It defines the performance characteristics and the minimum requirements of the instruments to be used. The lower and upper sizes considered within this document are 10 nm and a few micrometres, respectively. *In the CEN/TS 16976:2016, the lower limit of the measured particle size range was 7 nm. In the proposed standard, is set to be 10 nm and thus identical to MPSS (Mobility Particle Size Spectrometers) measurements (see CEN/TS 17434).*

Particle number size distribution (PNSD)

The CEN/TS 17434:2020 "Ambient air - Determination of the particle number size distribution of atmospheric aerosol using a Mobility Particle Size Spectrometer (MPSS)" has been prepared by the Technical Committee CEN/TC 264 "Air Quality", the secretariat of which is held by DIN. This document describes a standard method for determining the particle number size distribution in ambient air in the size range from 10 to 800 nm up total concentrations up to approximately 10^5 cm^{-3} with a time resolution of a few minutes. The standard method is based on a MPSS used with a bipolar diffusion charger and a CPC as the detector. The document describes the performance characteristics and minimum requirements of the instruments and equipment to be used and describes sampling, operation, data processing and QA/QC procedures including calibration.

3.1.2 Other relevant guidance

In addition to the aforementioned standards, there is a number of technical guidance and reports for measuring UFP PNC and PNSD, as those prepared by GAW and ACTRIS, providing recommendations, guidelines, standard operating procedures and scientific articles for aerosol in-situ measurements. These are openly available at ACTRIS (2024a, b, c). Some of these guidelines (with links), related to PNC and PMSD measurement, are listed in the "References" section. These documents provide guidance on Aerosol In-Situ Measurements, including aerosol inlets and conditioning (recommendations for aerosol drying, aerosol inlets and sampling tubes.)

3.2 Sampling and conditioning

Both standards provide detailed instructions regarding sampling and conditioning of air sample. Recommendations are very similar for the two measurements.

Additional information is provided by ACTRIS (2024a, b, c), where recommendations, guidelines, standard operating procedures and scientific articles for aerosol in-situ measurements are available.

Below we summarize some key points:

3.2.1 Sampling

The measuring instruments will be housed in a protected environment under controlled conditions (temperature 20 °C to 30 °C).

To measure particles in air quality, the air inlet must be between 1.5 m and 4 m above the ground, and up to 8 m in specific conditions (2008/50/CE). However, the CEN standards for UFP and PNSD suggest that the air inlet must be between 5 and 10 m above ground level, for measuring undisturbed atmospheric aerosols, and between 1.5 and 4 m for measuring aerosols close to the source. This inconsistency is related to the sampling requirements of different networks and their scopes such as air quality and regional/urban background.

To prevent the sampling lines from becoming contaminated with coarse particles, a PM10 or PM2.5 inlet is obligatory. prEN 16976:2023 recommends avoiding an inlet that removes particles in the CPC measurement range (e.g. PM1 or PM2.5). On the contrary, CEN/TS 17434:2020 recommends using an impactor or cyclone; D50=1 µm, as a pre-separator for measuring PNSD when the aerosol to be measured contains a significant number of coarser particles, while ACTRIS recommends a PM2.5 pre-separator.

It is necessary to minimize diffusional losses for ultrafine particles, and losses due to impaction and sedimentation for super-micrometre particles. According to CEN standards, the diffusion losses in the sampling system for 10 nm particles shall be < 25 %. It is recommended carrying out sampling with tubes as short as possible, avoiding bends and horizontal pipes. To minimize the losses of ultrafine particles by diffusion, the flow Reynolds number should be optimized. The flow must be laminar with a maximum Re of 2000.

Sampling tubes should be made of a conductive, corrosion-resistant material with a low surface roughness (e.g., stainless steel). Flexible tubing of electrically conductive material may also be used for small connections or short distances (<50 cm).

To reduce diffusion loss, it is necessary to intake aerosol with the aid of a pump at a primary flow rate, much higher than the secondary flow rate feeding the CPC. The primary flow should be laminar in order to prevent additional particle loss due to turbulence (Reynolds number of Re ≤ 2000).

It is recommended to use an isokinetic splitter to avoid over-or under sampling of super-micrometre particles.

The inlet and the flow-splitter shall be checked regularly to detect obstructions and cleaned, if necessary.

The pressure and temperature are need for the calculation of the concentration at “Standard Temperature & Pressure” (STP) requested by CEN standards, but concentrations are given in ambient conditions in air quality standards. Here there is another inconsistency.

3.2.2 Drying

The aerosol in-situ measurements should be done at a relative humidity lower than 40%. This is necessary to obtain comparable data, given that the size of hygroscopic particles is highly influenced by humidity.

Heating to reduce the relative humidity is not recommended, due to the loss of semi-volatile particles

The use of membrane dryer such as Nafion is the preferred method to dry the aerosol flow.

Use of aerosol diffusion dryers based on silica gel can produce high particle losses due to diffusion. This method is recommended in both CEN/TS 16976:2016 and CEN/TS 17434:2020, but is excluded in ACTRIS standard procedures and the prEN 16976:2023 the proposed standard, because diffusion losses are too high with this type of dryer.

At each instrument, the relative humidity, temperature, and pressure should be measured. RH should be measured in the inlet before and after the Nafion dryer.

3.2.3 Dilution

Dilution with dry particle-free air can be also applied to reduce humidity of the ambient aerosol

Moreover, dilution with particle-free air can be applied to reduce the number concentration of the ambient aerosol to the limits of the CPC's measuring range.

Dilution may introduce a high uncertainty, which shall be estimated. The exact dilution ratio shall be known in order to calculate the correct concentrations.

Operation principles of suitable dilution systems are presented in prEN 16976:2023.

3.2.4 Performance criteria and test procedures for the sampling and conditioning system

The standards list the performance criteria for the sampling system which shall be met in the performance tests, also specified. The following sampling system parameters shall be recorded unless they are covered by the CPC or MPSS data protocol:

- Relative humidity, temperature and absolute pressure at the CPC and MPSS inlet.
- Drying method (if applicable); primary or secondary flow.
- Dilution factor (if applicable).
- Status or primary flow pump.

Requirements:
- Particle losses due to diffusion: have to be determined and corrected for, based on equivalent lengths.
- Relative humidity of secondary flow at CPC inlet (<40% accuracy ±3%) and MPSS inlet (<40% accuracy ±5%).
- Dilution factor, if applicable; accuracy stable in time: ±5% for CPC, and ±6.5% for MPSS.
- Primary and secondary sampling flow laminar (Re ≤2000) accuracy ±10%.

3.3 Determination of the PNC (UFP)

The prEN 16976:2023 document describes a standard method for determining the particle number concentration in ambient air by using a CPC operated in the counting mode. The lower limit of the measured particle size range is set to be 10 nm and thus identical to MPSS measurements (see CEN/TS 17434). In air quality monitoring networks where MPSS will be used for determining the particle size distribution a CPC may be used for QA purposes for the MPSS data.

This standard provides detailed instructions regarding sampling and conditioning of air sample (see 5.2), the determination of the number concentration with a CPC, general requirements for the CPC performance criteria and test procedures for the CPC and the sampling system. Also, comprehensive description is provided for the measurement procedure and QC/QA and measurement uncertainty.

We refer the reader to the original standard. Below we summarize the most important topics.

3.3.1 Method of operation for determining PNC

In a CPC, particles are enlarged by **condensation growth** and then subjected to optical detection by scattered light.

The aerosol is saturated at constant temperature with a vapor substance (e.g. butanol) in a heated saturator. It is then cooled, and the vapor condenses on the particles, forming spherical droplets a few micrometres in diameter. These droplets, can be easily detected and counted optically. Thus, the aerosol droplets are illuminated by a light beam, and the light scattered under a defined angle is conducted to a photodetector.

If the particle number concentration is sufficiently low, the droplets pass through the light beam one after another, thus generating individual electrical pulses at the detector output. For higher concentrations there may be more than one particle at the same time in the measurement volume, which produces a coincidence error that results in a measured value lower than the true concentration, and which can be corrected. For even higher concentrations, the detector measures the light scattered by the entire particle population as an analogue photometer signal (photometric mode). In principle, there is a linear relationship between this photometer signal and the particle number concentration. However, the error can be very high, so the proposed standard does not allow the use of the photometric mode.

ACTRIS (2024c) reports the in-situ instruments in compliance for aerosol measurements.

3.3.2 CPC performance criteria and test procedures

The CEN standard lists the performance criteria for the sampling system and for the CPC. The standard sets out the following general requirements for the CPC:

- All the performance criteria refer to the counting mode of the CPC.
- Coincidence correction and the calibration factor shall be applied.
- The CPC shall have no internal flow splitting, which is not accessible to an external flow rate check, or internal dilution to avoid unnecessary sources of measurement uncertainty.
- The working fluid shall be n-butanol.
- The instrument shall produce concentration data averaged over a data reporting interval of 1 min.
- The instrument's internal clock shall be externally synchronisable.
- The instrument shall enable the following parameters to be recorded in 1 min time intervals:
  - Date, start time and end time of each reported concentration.
  - Analysed flow rate.
  - Raw concentration (count rate divided by the analysed flow rate), in cm^{-3}.
  - Concentration with internal coincidence correction (based on the analysed flow rate), in cm^{-3}.
  - Saturator temperature, in K.
  - Condenser temperature, in K.
  - Temperature and absolute pressure at the point of flow rate measurement.
  - Warning and error flags.

3.3.3 Measurement procedure

Standard provides recommendation for measurement planning, installation, and initial checks on-site.

3.3.4 Quality control, quality assurance and measurement uncertainty

Maintenance, checking and calibration procedures to be follow are specified in the standard. This includes checking of the final data.

General operating procedures: maintenance of CPC, calibration of linearity, determination of the efficiency curve, flow and sensors checks, internal diagnostics, etc.

QA/QC procedures and criteria to the measurement of uncertainty are provided.

Minimum frequency of recommended calibrations, checks and maintenance operations are suggested for CPC long-term monitoring, including CPC and sampling system.

There are several sources of uncertainty such as the detection efficiency of the CPC (size and material dependent), particle losses in the sampling system, flow determination, unaccounted humidity, etc.

3.4 Determination of the PNSD

The CEN/TS 17434:2020 describes a standard method for determining the particle number size distribution in ambient air in the size range from 10 to 800 nm for total concentrations up to 10^5 cm^{-3}, with a time resolution of a few minutes. The standard method is based on a MPSS used with a bipolar diffusion charger and a CPC as the detector. The document describes the performance characteristics and minimum requirements of the instruments and equipment to be used and describes sampling, operation, data processing and QA/QC procedures including calibration.

The standard provides detailed instructions regarding sampling and conditioning of air sample, the determination of the particle number size distribution with a MPSS, general requirements for the MPSS, performance criteria and

test procedures for the MPSSs and the sampling system. Also, a comprehensive description is provided for the measurement procedure and QC/QA and measurement uncertainty. **We refer the reader to the original standard. Below we summarize the most important topics.**

3.4.1 Method of operation for determining PNSD with a MPSS

The MPSS consists of a bipolar diffusion charger, a differential mobility analyser (DMA) and a CPC.

First the aerosol particles are brought to a bipolar charge balance by a bipolar diffusion charger, which can be a radioactive or soft X-ray source. The bipolar diffusion charger continuously generates positive and negative ions. When radioactive sources are used (e.g. ^{85}Kr, ^{63}Ni, ^{241}Am and ^{210}Po), a bipolar distribution is assumed according to ISO 15900. When other ionizers are used (e.g. X-ray), an adapted bipolar charge distribution must be applied (Note: the bipolar charge distribution might be different for different models).

The bipolarly charged polydisperse aerosol is injected into a DMA. By setting different voltages on the DMA, particles with different electrical mobility are selected, which mainly depends on the number of elementary charges of the particles and their diameter. Increasing or decreasing the voltage produces an electrical particle mobility distribution.

After passing through the DMA, the particle number concentration is measured by a CPC (that shall meet the requirements defined in CEN/TS 16976) at several different voltages covering the entire range of electric particle mobility to be investigated.

After passing through the DMA, the particle number concentration is measured by a CPC (meeting the CEN/TS 16976 requirements) at different voltages, covering the entire range of mobility of the electrical particles at investigate.

Finally, determining the particle number size distribution requires a data inversion process that considers size-dependent charging probabilities.

3.4.2 Correction for particle losses due to diffusion

The total losses of particles by diffusion in the instruments and in the sampling, lines must be determined as a function of the size of the particles. Commercial instruments provide correction software for particle losses due to diffusion, but do not correct for particle losses due to diffusion in the sampling system. In order to harmonize the reported measurement data, the standard recommends applying a common method for correction of particle losses due to diffusion based on equivalent length. In Wiedensohler et al. (2012) this method is introduced for the correction of the number size distribution.

3.4.3 Correction for CPC detection efficiency

The particle number concentration in each size class, for which the detection efficiency is lower than one, has to be divided by the corresponding detection efficiency value to get the corrected number concentration.

3.4.4 MPSS performance criteria and test procedures

The CEN standard sets out the requirements for the MPSS design and performance. We summarize some of them below:

- The obligatory particle size range is defined to 10-800 nm (the size range could be extended to larger particles sizes if the MPSS allows this).
- Pre-separator is only necessary if the aerosol to be measured contains a significant number concentration of particles large that the upper size limit of the MPSS.

- Bipolar diffusion charger: When radioactive sources are used (e.g. ^{85}Kr, ^{63}Ni, ^{241}Am and ^{210}Po), a bipolar distribution is assumed according to ISO 15900. When other ionizers are used (e.g. X-ray), an adapted bipolar charge distribution must be applied.
- DMA: Sheath air will be filtered (HEPA filter) and dried; temperature and relative humidity shall be measured; Sheath air <40% at DMA outlet.
- Capability of independently measuring the voltage output is recommended.
- Capability of performing upscan and downscan with a high size resolution at least for calibration.
- CPC shall meet the requirements defined in prEN16976.
- The particle size resolution of 16 to 32 geometrically equal distributed size channels per size decade.
- Time to measure a particle number size distribution between 2 and 10 minutes.

The CEN standard also sets out the requirements for the MPSS performance:

- Actual aerosol flow rate ≤5 % difference to the nominal flow rate.
- Particle size accuracy ≤3 % at one size between 100 nm and 300 nm.
- Accuracy of the integrated particle number concentration measurement, by comparison with a reference CPC (CEN/TS 16976), connected to the same sampling line, over a period of at least 8 hours: 0.9 ≤ slope ≤ 1.1 (forced through the origin R^2≥0.9.)
- Integral number concentration <0.01 cm^{-3} for a 10 min measurement of HEPA filtered air.
- Inlet flow should be laminar flow.
- Accuracy of the particle number size distribution shall be determined experimentally by a comparison against a reference MPSS integrated particle number concentration by comparison with a reference CPC (CEN/TS 16976) connected to the same sampling line: deviation ≤10% for size channels between 20 nm and 200 nm, ≤50 % for 10 nm to 20 nm, and ≤20 % for 200 nm to 800 nm.

3.4.5 Measurement procedure

Standard provides recommendation for measurement planning, installation, and initial checks on-site.

3.4.6 Quality control, quality assurance and measurement uncertainty

Frequent services and calibrations are important, but external calibrations are also very important are strongly recommended. TROPOS is doing these external calibrations for ACTRIS supersites (Wiedensohler et al., 2018).

Maintenance, checking and calibration procedures to be follow are specified in the standard. This includes checking of the final data.

General operating procedures: cleaning of DMA, cleaning of the saturator and optics of CPC, etc. are listed.

QA/QC procedures and criteria to the measurement of uncertainty are provided.

Minimum frequency of recommended calibrations, checks and maintenance operations are suggested for MPSS long-term monitoring, including MPSS and sampling system.

The measurement uncertainty of particle number size distribution is very complex. There are two main components: the uncertainty in the particle number concentration for each size bin and the uncertainty in the particle size that is assigned to each of the size bins. There are several sources of uncertainty such as the detection efficiency of the CPC (size and material dependent), particle losses in the sampling system, uncertainties and instabilities of the aerosol and sheath flows, unaccounted humidity, DMA voltage, etc.

3.5 Data management

Regarding data reporting, in addition to the variables measured by CPC number concentration (PNC) and MPSS (number size distribution and particle diameter), complementary data, such as several flow and sampling system

parameters, shall be reported, as a minimum, at the same time resolution. These parameters are detailed in the corresponding CEN standards.

Moreover, both standards recommend to report data following EBAS protocols EBAS (2024), as detailed in ANNEX C of prEN 16976:2023 for reporting PNC and in ANNEX G of the CEN/TS 17434:2020).

The EBAS database, a major archive for data on atmospheric constituents worldwide, hosting data of different research programmes and infrastructures such as European Monitoring and Evaluation Programme (EMEP) or the WMO Global Atmosphere Watch (GAW) programme, among others.

EBAS has defined, in collaboration with EUSAAR and the EU Infrastructure ACTRIS (Aerosols, Clouds, and Trace gases research infrastructure), common standard operating protocols and data reporting procedures for observations of atmospheric aerosol properties. These protocols and procedures have been adopted by the WMO GAW programme.

Although other protocols are feasible, they have been adopted by a large scientific community and have been operative during the last decade. RI-URBANS has collected PNC and PNSD data from air quality monitoring networks (which had not previously provided data to EBAS database) and has adapted the datasets to the EBAS requested formats, making data available to the scientific community in EBAS.

In order to meet the needs of different network architectures, EUSAAR, ACTRIS and GAW defined 3 data levels and corresponding data file formats: Level 0, Level 1, and Level 2.

Level 0: this format contains **raw data** values and instrument state parameters at the instrument's **native temporal resolution** (usually minute resolution). The level 0 data are already calculated particle number concentrations for the CPC and MPSS. Volume concentrations are expressed in the internal temperature and pressure conditions of the instrument.

Level 1: **data processed**, in the original temporal resolution, to final aerosol variable, i.e. particle number concentrations, or particle number size distribution. Potential corrections are applied (i.e. flow correction, size dependent counting efficiency…).

Level 2: **hourly averages**; concentrations are stated for standard temperature and pressure conditions (273.15 K; 1013.25 hPa). 15.87th and 84.13th percentiles for each averaging period.

Data, metadata and flags to be reported for each Level are indicated in prEN 16976:2023 and CEN/TS 17434:2020.

4. PAN-EUROPEAN OVERVIEW OF UFP AND PNSD ACROSS URBAN ENVIRONMENTS

4.1 Introduction

It is widely recognised that exposure to PM negatively impacts human health (WHO, 2013, 2021a). Several studies have also shown that UFP can penetrate deeply into the respiratory system, thus causing respiratory and cardiovascular diseases in humans (Cassee et al., 2019 and references therein). In the range <10 nm, a rapidly increasing fraction of particles are lost by diffusion in the nose, oral cavity, and trachea. The sizes UFPs not only allows them to reach the deeper parts of the respiratory system, but a fraction of these, reaching the alveoli, translocate and reach the circulatory system, and from there can reach any organ in the body, or directly reach the brain by translocating the olfactory bulb of the brain (Cassee et al., 2019, and references therein). The new World Health Organization Air Quality Guidelines (WHO, 2021b) identify UFP concentration as a relevant air quality parameter and find that, although there is a body of evidence for the health effects of UFPs, results are still inconsistent. Cassee et al. (2019) and Rivas et al. (2021) reported that this inconsistency may be, at least in part, due to methodological differences in measurements, to the lack of representation of UFP human exposure to UFPs resulting from the use of only a single monitoring station per city in most studies, and the different sources

contributing to UFP concentrations in other cities/regions. Although the WHO (2021b) does not provide guideline values, the monitoring of concentrations of UFPs and black carbon (BC) is recommended to allow a more accurate evaluation of their health effects.

UFP source apportionment based on UFP-PNSD measurements have typically reported sources of UFP including photochemical nucleation, several traffic sources (spark-ignition and compression-ignition), domestic and residential heating, regional secondary inorganic aerosols (i.e. regional nitrate and sulphate), particles associated with oxidants as represented by O_3 (i.e. regional secondary organic and inorganic aerosols) and other sources (such as biomass burning, urban background sources, industrial emissions, mixed sources, dust and unknown sources) (Hopke et al., 2022). Shipping and aviation might also contribute to increasing UFP concentrations with a prevalence of the lowest mode (Diesch et al., 2013; Lorentz et al., 2019; Stacey et al., 2021). When focusing on European urban background and traffic sites, traffic UFP contributions dominate PNC (with size modes around 10-20 and 70-90 nm), followed by photochemical nucleation or new particle formation (NPF, <20 nm), with NPF varying widely according to the climatic region (i.e., it is usually higher in the high-insolation areas; but not consistently) (Brines et al., 2015; Rivas et al., 2021). Other relevant source contributions include urban and regional background UFPs (usually with 80-150 nm modes).

Long-term measurements of UFP-PNSD are difficult when data coverages >90% are required. Although it can be done. Hopke et al. (2024) and Vörösmarty et al. (2024) carried out studies that cover 15 and 11 years of data, respectively, with a high data coverage. Also, data coverage reported by Trechera et al. (2023) for sites from Budapest, Helsinki, Ispra, Leipzig, Mulheim, Paris, Rochester, reached >90% data coverage but the other did not. The prior chapters show the complexity of accurately measure PNSD.

The lack of harmonisation for air quality between these measurements (both in terms of instrumentation and measurement conditions) makes the direct comparison of UFP-PNSD data from different cities very difficult.

In RI-URBANS, Trechera et al. (2023) compiled existing UFP-PNSD measurements in urban Europe for a joint evaluation according to (i) the instrumental and methodological approaches implemented; (ii) the comparison of urban concentrations across Europe; (iii) the identification of similarities and major differences; and (iv) the evaluation of relationships with other pollutants, such as BC, PM_x (PM_{10}, $PM_{2.5}$, PM_1), and gaseous pollutants (SO_2, NO_x, O_3, CO), and with meteorological parameters. In this section we summarise and update the results of this study. Furthermore, Liu et al. (2023) and Garcia-Marlès et al. (2024a) analysed these datasets to calculate and evaluate aerosol Lung Deposited Surface Area (LDSA) concentration and the 2009-2019 UFP-PNSD trends. The results from these RI-URBANS studies are also summarised. In Garcia-Marlès et al (2024b) the source apportionment of UFP-PNSD in 24 (mostly) urban sites is presented. There is also an additional guidance chapter on ST for UFP-PNSD in the website of RI-URBANS.

4.2 Methodology

4.2.1 UFP-PNSD Data compilation

This study is based on 29 2017-2019 UFP-PNSD datasets provided by air quality monitoring networks and research supersites (such as those from ACTRIS) to RI-URBANS. These include (Figure 1 and Table 1):

- Eighteen urban background (UB) sites covering most of Europe: Antwerp (ANT), Athens (ATH), Barcelona (BCN), Birmingham (BIR), Budapest (BUD), Dresden (DRE), Granada (GRA), Helsinki (HEL), Langen (LAN), Lecce (LEC), Leipzig (LEI), two in London (LND and LND2), Madrid (MAD), Marseille (MAR), Mülheim (MUL), Zürich (ZUR), and Rochester (ROC) in New York state in US.
- Six traffic (TR) sites in Central (C), West (W) and North (N) Europe: DRE, HEL, two in LEI (LEI and LEI2), LND and Stockholm (STO), but not in South (S) Europe.
- Four suburban background (SUB) sites: ATH, Lille (LIL), Paris (PAR) and Prague (PRA).

- One regional background (RB) site in the Po Valley in Italy (Ispra, ISP), was included because no datasets could be obtained from urban areas in the Po Valley, and this is a pollution hotspot in Europe, where most of the PM pollution has a regional origin.

This period was selected to obtain relatively recent data, without the effect of the decrease of pollution due to the COVID-19 lockdown-associated measures, which were variable across urban Europe and globally (Putaud et al., 2021; Torkmahalleh et al., 2021).

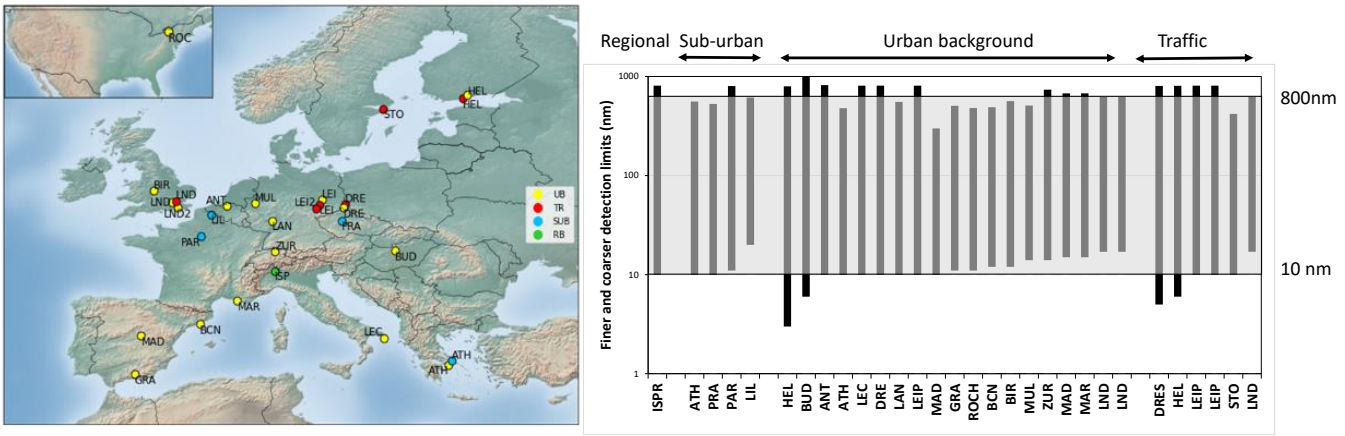


Figure 1: *Left: Location of the cities supplying data on particle number concentrations and size distributions for the present study and the type of station. UB, Urban background; TR, Traffic; SUB, Suburban background; RB, Regional background. Right: Particle size detection limits of PNSD measurements of this study and recommended ones from CEN (10-800 nm). Modified from Trechera et al. (2023).*

Table 1: *List of air quality sites supplying UFP-PNSD datasets to this study with location, type of environment, equipment used and particle size range used in this study. UB, Urban Background; TR, Traffic; SUB, Suburban Background; RG, Regional Background. TRO, TROPOS; LDMA, long DMA; VDM, Vienna type DMA; AIRM, Airmodus. Modified from Trechera et al. (2023).*

City (Country)	Station Name	Type	Acronym	Coordinates	Equipment	
Antwerp (BE)	Borgerhout	UB	**ANT_UB**	51.21N, 4.43E	SMPS Grimm C5420 L-DMA	10-808
Athens (GR)	Thissio	UB	**ATH_UB**	38.00N, 23.72E	SMPS TSI 3080L, CPC TSI 3772	10-470
Barcelona (ES)	Palau Reial	UB	**BCN_UB**	41.39N, 2.13E	SMPS TSI 3080, CPC TSI 3772	12-478
Birmingham (GB)	BAQS	UB	**BIR_UB**	52.46N, 1.93 W	SMPS TSI 3082., CPC TSI 3750	13-552
Budapest (HU)	CAAG	UB	**BUD_UB**	47.48N, 19.06E	DMPS, CPC TSI 3775	11-816
Dresden (DE)	Winckelmann.	UB	**DRE_UB**	51.04N, 13.73E	TRO-TSMPS VDMA 28, TSI 3010/3772	10-800
Granada (ES)	UGR	UB	**GRA_UB**	31.18N, 3.58 W	SMPS TSI 3082, CPC TSI 3772	11-496
Helsinki (FI)	SMEARIII	UB	**HEL_UB**	60.12N, 24.58E	TDMPS Hauke-DMA, CPCTSI 3025	10-794
Langen (DE)	UBA	UB	**LAN_UB**	50.00N, 8.39E	SMPS TSI 3080, TSI 3772, TRO rebuild	10-544
Lecce (IT)	Lecce Obs.	UB	**LEC_UB**	40.20N, 18.07E	TRO-MPSS	10-800
Leipzig (DE)	TROPOS	UB	**LEI_UB**	51.35N, 12.43E	TRo-TDMPS VDMA, UCPC TSI 3025	10-800
London (GB)	N.Kensington	UB	**LND_UB**	51.52N, 0.21 W	SMPS TSI 3080, CPC TSI 3775 LDMA	17-604
London (GB)	Honor Oak P.	UB	**LND2_UB**	51.45N, 0.04 W	SMPS TSI 3080, CPC TSI 3775 LDMA	17-605
Madrid (ES)	CIEMAT	UB	**MAD_UB**	40.45N, 3.73 W	SMPS TSI 3080L, CPC TSI 3775	15-661
Marseille (FR)	Longchamp	UB	**MAR_UB**	43.31N, 5.39E	SMPS TSI LDMA 3081A, CPC TSI 3752	15-661
Mülheim (DE)	Styrum	UB	**MUL_UB**	51.45N, 6.87E	SMPS TSI 3080, CPC TSI 3772	14-496
Rochester US)	NYS DEC	UB	**ROC_UB**	43.15N, 77.55 W	SMPS TSI 3071, CPC TSI 3010	11-470
Zurich (CH)	Kaserne	UB	**ZUR_UB**	47.38N, 8.53E	SMPS TSI 3034, Nafion dryer	17-478
Dresden (DE)	North	TR	**DRE_TR**	51.09N, 13.76E	TROPOS-SMPS VDMA, CPC TSI 3772	10-800
Helsinki (FI)	Mäkelänkatu	TR	**HEL_TR**	60.19N, 24.95E	UHEL DMPS VDMA, CPC AIRM A20	11-800
Leipzig (DE)	Mitte	TR	**LEI_TR**	51.34N, 12.38E	TRO-TDMPS VDMA, UCPC TSI 3025	10-800
Leipzig (DE)	Eisenbahn	TR	**LEI2_TR**	51.35N, 12.41E	TRO-TDMPS VDMA, UCPC TSI 3025	10-800
London (GB)	Marylebone	TR	**LND_TR**	51.52N, 0.15 W	SMPS TSI 3080, CPC TSI 3775 LDMA	17-604
Stockholm (SE)	Hornsgatan	TR	**STO_TR**	59.32N, 18.05E	SMPS TSI 3071, CPC TSI 3775	10-410
Athens (GR)	Demokritos	SUB	**ATH_SU**	37.99N, 23.82E	SMPS TSI 3080, CPC TSI 3772	10-550
Lille (FR)	V. d'Ascq	SUB	**LIL_SUB**	50.61N, 3.14E	SMPS TSI 3082, CPC TSI 3750	20-594
Paris (FR)	SIRTA	SUB	**PAR_SUB**	48.71N, 2.16E	SMPS GRIMM 5416, OPC GRIMM	11-792
Prague (CZ)	Schudol	SUB	**PRA_SUB**	50.13N, 14.38E	SMPS TSI 3034 TRO rebuilt	10-519
Ispra (IT)	JRC	RG	**ISP_RB**	45.80N, 8.63E	DMPS VDMA, CPC TSI 3010/3772	10-808

4.2.2 2009-2019 trend analysis of UFP-PNSD

The instrumentation used for measuring UFP-PNSD and BC at the different stations is reported in Table 2. The instruments used are the Scanning Mobility Particle Sizer (SMPS), Differential Mobility Particle Sizer (DMPS), Twin Scanning Mobility Particle Sizer (TSMPS) or Twin Differential Mobility Particle Sizer (TDMPS) (Table 1). Some stations start measuring PNSD at finer sizes (HEL_UB and HEL_TR, 3 and 6 nm, respectively; DRE_TR, 5 nm; BUD_UB, 1000 nm) or end at coarser upper limits (HEL_UB and TR, 891 nm; BUD_UB, 1000 nm). Nevertheless, the latter affects total PNC to a lower degree than the first because of the relatively low PNC within the coarser sizes. Furthermore, several sites start size measurements from 11 to 20 nm (BCN_UB, BIR_UB, GRA_UB, LIL_SUB, the three sites from LND, MAR_UB, MUL_UB, PAR_SUB, ROC_UB and ZUR_UB), instead of the recommended 10 nm; or end with lower coarser sizes, instead of the recommended 800 nm.

Garcia-Marlès et al. (2024a) carried out the trend analysis of 2009-2019 datasets covering at least 5 years to detect monotonic trends over the time using the non-parametric Theil-Sen method (Sen, 1968; Theil, 1992). This method, robust against outliers, is commonly applied for air quality data analysis (Carslaw and Ropkins, 2012). The magnitude of the trends was quantified by the Theil–Sen slope, which is the median of all the possible slopes between the data pairs and the statistical significance (ss) was also evaluated. These analyses were conducted using the Openair package. It should be noted that some of the time series are relatively short for the discernment of trends, and some of the longer time series show different gradients dependent upon the time interval selected. The individual slopes, expressed as a percentage change per year with their 95% confidence interval, were summarised using random-effects meta-analysis due to the large heterogeneity of the data between the included sites (Chen and Peace, 2013). The mean effect was calculated for each class of site individually (urban, suburban, regional and traffic sites) as well as globally to provide a comprehensive overview of the results. Meta-analyses were carried out using the "meta" R package version 6.5-0 (Balduzzi et al., 2019).

4.2.3 Determination of lung deposited surface area (LDSA) from UFP-PNSD

The 29 UFP-PNSD datasets collected between 2017-2019 were analysed to estimate the regional deposition of LDSA in the head/throat (HA), tracheobronchial (TB), and alveolar (ALV) regions of the human respiratory system. LDSA concentrations can be measured directly (Nanoparticle Surface Area Monitor, NSAM, Reche et al. 2015 or Pegasor LDSA sensor, Kuula et al. 2019) or calculated from the PNSDs measured. In RI-URBANS we used data from PNSD measurements. The method commonly used to determine the geometric surface area concentration of spherical particles is based on the measurement of PNSD. In our calculations, we used size-dependent regional deposition fraction (DF) curves obtained from MPPD software (version 3.04, Chemical Industry Institute of Toxicology, Research Triangle Park, NC. The total LDSA values were calculated by first counting the number of particles in each size bin and then multiplying the PNC with the specific deposition fraction of the given particle size. To accurately assess the contributions of LDSA, it is important to consider the particle sizes involved. Particles < 10 nm have a relatively low weight in the overall calculation of LDSA contributions (0.14% ± 0.2%), compared to other particle sizes.

4.3 Concentrations of UFP and PNSD

Only 18/29 datasets had >70% data availability in 2017-2019 and 7/29 had data availability of <50%. This deficiency reflects the complexity of the UFP-PNSD measurements and the need for detailed supervision and frequent instrumentation maintenance. Furthermore, to increase comparability, this study evaluated the $N_{10\text{-}800}$ concentrations. In any case, when comparing PNC, one should consider site-specific lower detection sizes. For instance, $N_{20\text{-}594}$ (LIL_SUB) and $N_{10\text{-}800}$ (HEL_UB) were compared as $N_{10\text{-}800}$= PNC, despite their different sizes.

Table 2 summarises the averaged, PNC ($N_{10\text{-}800}$), and $N_{10\text{-}25}$, $N_{25\text{-}100}$ and $N_{100\text{-}800}$ for the 29 study sites.

4.3.1 Particle number size distributions

Figure 2 shows the UFP-PNSD data, which were classified into the following four groups:

- **TR sites** (DRE, HEL, LEI, LEI2, STO, LND), with high PNC, and, very frequently, with the highest values in the Nucleation mode due to freshly emitted and quickly nucleated particles from traffic exhaust emissions (Harrison et al., 2011; among others).
- **UB sites from southern, central and eastern Europe** (ANT, ATH, BCN, BUD, GRA, LAN, LEC, LEI, MAD, MAR, MUL), with most of the sites recording also high PNCs, but very variable PNSD.
- **UB sites from northern and central Europe, UK and northern US** (BIR, DRE, HEL, LND, LND2, ROC, ZUR), with relatively low PNCs and a prevalent Aitken mode size (30-40 nm) indicating traffic influence, with a relatively high load of the Nucleation mode in the cases of DRE, HEL and ROC.
- **SUB and RB sites** (ATH, LIL, PAR, PRA, ISP similar to the UB sites in northern Europe but with a slightly coarser prevalent mode (50 nm, indicating growth by ageing).

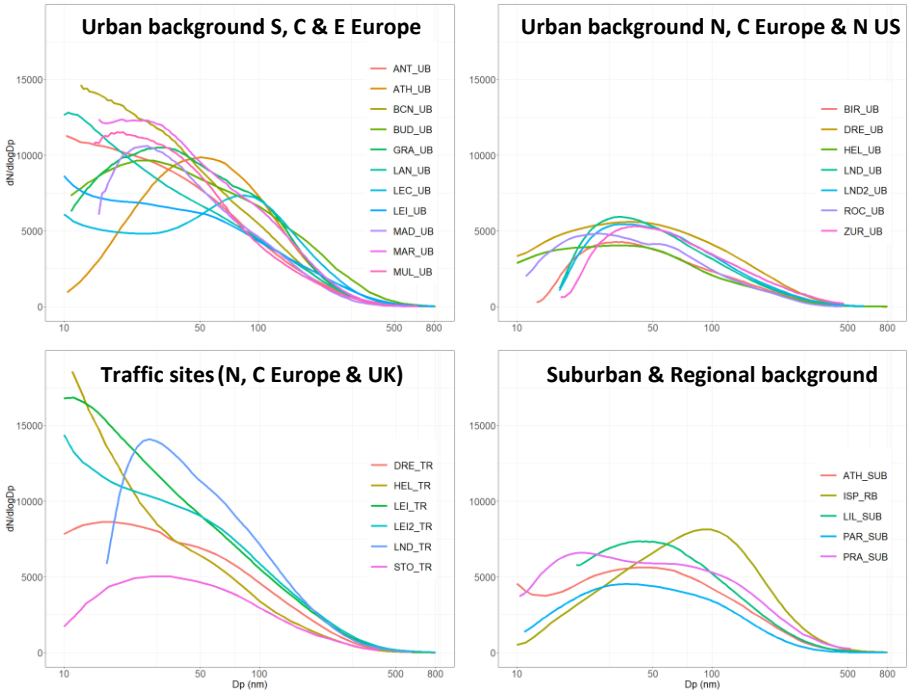


Figure 2: *Averaged 2017-2019 particle number size distributions for Traffic, Urban background sites from S, C and E Europe, Urban background from N, C Europe, UK and N US, and Suburban and Regional background sites. Modified from Trechera et al. (2023).*

4.3.2 Particle number concentrations

Focusing on UB sites, the highest PNCs were recorded in eastern and southern Europe (BCN, BUD, GRA and MAR, 11200 to 10300 # cm^{-3}) and two central European sites (ANT and LAN, close to 10000 # cm^{-3}), followed by central-southern Europe (MUL, ATH, LEC, LEI, MAD and DRE, 8900 to 6200 # cm^{-3}) and north and north-western Europe and Switzerland (LND, LND2, ROC, HEL, ZUR and BIR, 4500 to 3500 # cm^{-3}) (Figure 3). The TR sites record high PNCs, with 13500 to 10500 # cm^{-3} at the LEI, LEI2, LND and HEL sites; followed by 8800 and 5100 # cm^{-3} at DRE and STO (Table 2 and Figure 3), but there are no TR sites supplying UFP-PNSD data in S and E Europe. As it could be expected, the SUB and RB sites recorded relatively low concentrations, with 7400 to 4500 # cm^{-3} (Figure 3). When the $N_{25\text{-}800}$ showed a similar pattern to BC (Figure 3), with a clear decreasing trend from northern to southern Europe. In all cases (BC, PNC and N25-800), and for a specific climate region, concentrations decrease as follows: TR>UB>SUB.

Table 2: *UFP-PNSD arithmetic averages concentrations and their standard deviations, containing Nucleation, Aitken and Accumulation mode (N_{10-25}, N_{25-100} and $N_{100-800}$, respectively), N_{25-800} and PNC (N_{10-800}) from all different stations collected in RI-URBANS. ND, Not-determined; UB, Urban Background; TR, Traffic; SUB, Suburban Background; RG, Regional Background. Modified from Trechera et al. (2023).*

Station Name	N_{10-25} # cm^{-3}	σ_{10-25} # cm^{-3}	N_{25-100} # cm^{-3}	σ_{25-100} # cm^{-3}	N_{10-100} # cm^{-3}	σ_{10-100} # cm^{-3}	$N_{100-800}$ # cm^{-3}	$\sigma_{100-800}$ # cm^{-3}	N_{25-800} # cm^{-3}	σ_{25-800} # cm^{-3}	N_{10-800} # cm^{-3}	σ_{10-800} # cm^{-3}
ANT_UB	4466	3141	4322	2612	8788	5025	1269	951	5591	3272	10057	5510
ATH_UB	1503	1312	5338	4642	6841	5448	1711	2060	7049	6393	8552	7064
BCN_UB	4245	4141	5560	3820	9805	6641	1380	901	6940	4441	11186	7481
BIR_UB	661	632	2197	1813	2858	2263	673	647	2871	2318	3532	2725
BUD_UB	3691	3075	4973	3333	8664	5785	2173	1465	7146	4408	10837	6653
DRE_UB	1935	2322	3038	2529	4973	4019	1242	1000	4280	3236	6215	4524
GRA_UB	3129	2677	5629	4160	8758	6230	1776	1431	7406	5395	10535	7305
HEL_UB	1419	1526	2144	1764	3563	2913	644	507	2789	2056	4208	3119
LAN_UB	4628	4491	4074	2762	8702	5890	1254	888	5328	2999	9956	6657
LEC_UB	2293	2822	3590	2741	5883	4470	2072	1907	5662	4355	7954	5637
LEI_UB	3236	4076	3524	2818	6760	5691	1403	1067	4928	3528	8163	6093
LND_UB	614	560	2983	2433	3597	2790	891	1003	3874	3223	4489	3535
LND2_UB	540	405	2912	2256	3452	2509	964	999	3875	3106	4415	3316
MAD_UB	1997	1908	4806	3632	6803	4942	1134	923	5940	4313	7937	5702
MAR_UB	2679	1760	5894	3881	8573	5160	1723	1539	7618	5161	10297	6274
MUL_UB	2810	2139	5058	3375	7868	4955	1062	804	6120	3855	8930	5351
ROC_UB	1434	1428	2370	1849	3804	2867	602	430	2973	2105	4407	3076
ZUR_UB	296	264	2845	2156	3141	2336	1061	707	3905	2696	4201	2860
DRE_TR	3647	2939	3892	2499	7539	4655	1252	809	5144	3077	8791	5051
HEL_TR	6091	6704	3357	2816	9448	8698	1009	704	4366	3322	10457	9088
LEI_TR	6711	5725	5272	3062	11983	7750	1580	936	6852	3696	13563	8134
LEI2_TR	5249	5252	5075	3368	10324	7331	1699	1142	6774	4217	12023	7860
LND_TR	1961	1270	6753	3943	8714	5045	1900	1261	8653	5016	10614	6070
STO_TR	1646	1441	2756	1807	4402	2848	653	416	3409	2005	5056	3016
ATH_SUB	1654	2749	3245	2469	4899	4561	1203	725	4449	2923	6103	4892
LIL_SUB	560	625	4148	2829	4708	3230	1421	1103	5569	3557	6129	3890
PAR_SUB	1022	1055	2567	1997	3589	2789	876	708	3443	2510	4465	3241
PRA_SUB	2209	2689	3722	2636	5931	4471	1508	1101	5230	3312	7439	4875
ISP_RB	996	1231	4058	2459	5054	2924	2319	2133	6377	4189	7373	4351

4.3.3 Nucleation, Aitken and Accumulation modes

As stated above Nucleation mode particles might arise from photochemical nucleation and from traffic emissions. For datasets with a lower size detection limit of 13 nm, the highest Nucleation mode proportions in PNC were reached at the TR sites (42-58%, excluding STO, 33%). For UB sites, the lowest proportions were reached in ATH and BIR (18 and 19%, respectively), intermediate proportions (29-34%) in LEC, GRA, BUD, MUL, HEL and DRE, and the highest proportions (38-46%) in BCN, LEI, ANT and LAN. Consequently, for the UB: (i) the highest proportion of Nucleation mode concentrations was reached not only at sites from southern Europe, but especially in central Europe (LEI and LAN); and (ii) one southern Europe site (ATH) had the lowest proportions due to the high condensation sink and the low NH_3 in this urban area (Vratolis et al., 2019). Aitken mode proportions reached 32-44% of PNC at the TR sites, excluding STO with 54%; 41-54% at the UB sites (with the highest at BIR and ATH, both 62%); and 48-57% at all SUB and RB sites. Accumulation mode proportions for PNC reached only 10-20% in all evaluated datasets, excluding ISP_RB at 31%.

Nucleation mode (N_{10-25})

The absolute Nucleation mode concentrations were lower at the SUB (1000-2200 # cm^{-3}) and RB (1000 # cm^{-3}) sites and markedly higher at the UB (most in the range 1500-4600 # cm^{-3}) and TR sites (most in the range 3600-6700 # cm^{-3}). Considering only UB sites, N_{10-25} were higher in central, eastern and southwestern Europe (2800-4600 # cm^{-3}, excluding DRE, 1900 # cm^{-3}) and lower in northern and south-eastern Europe and N US (700-1500 # cm^{-3}). The highest UB Nucleation mode concentrations were recorded at the following sites in the order: LAN>ANT>BCN>BUD>LEI>GRA>MUL>LEC>DRE>ATH>ROC>HEL. Therefore, as previously stated, it is not the case that southern Europe (with higher insolation) records the highest concentrations of the Nucleation mode, but the contribution of other sources and processes probably significantly contributes to increasing the finest UFPs, especially in central and eastern Europe (see Junkermann et al., 2016).

Aitken mode (N_{25-100})

For the Aitken mode, all twenty-seven datasets were considered since all sites started measurement at lower sizes than 25 nm. Small differences were found between the Aitken mode concentrations obtained at TR sites (2800-6800 # cm^{-3}) and those obtained at UB (2100-5900 # cm^{-3}), SUB (2600-4100 # cm^{-3}) and RB (4100 # cm^{-3}) sites. However, in the last case, the reader must consider that ISP is located in the Po Valley. The lack of data from TR sites in southern and eastern Europe makes it difficult to compare concentrations at TR versus UB sites across Europe. However, for UB sites, marked regional trends were again found, with the highest concentrations in southern Europe (4800-5900 # cm^{-3}), intermediate concentrations in central Europe (2800-5100 # cm^{-3}) and the lowest concentrations in northern, north-western Europe (2100-3000# cm^{-3}); again, this runs parallel to the air pollution trends.

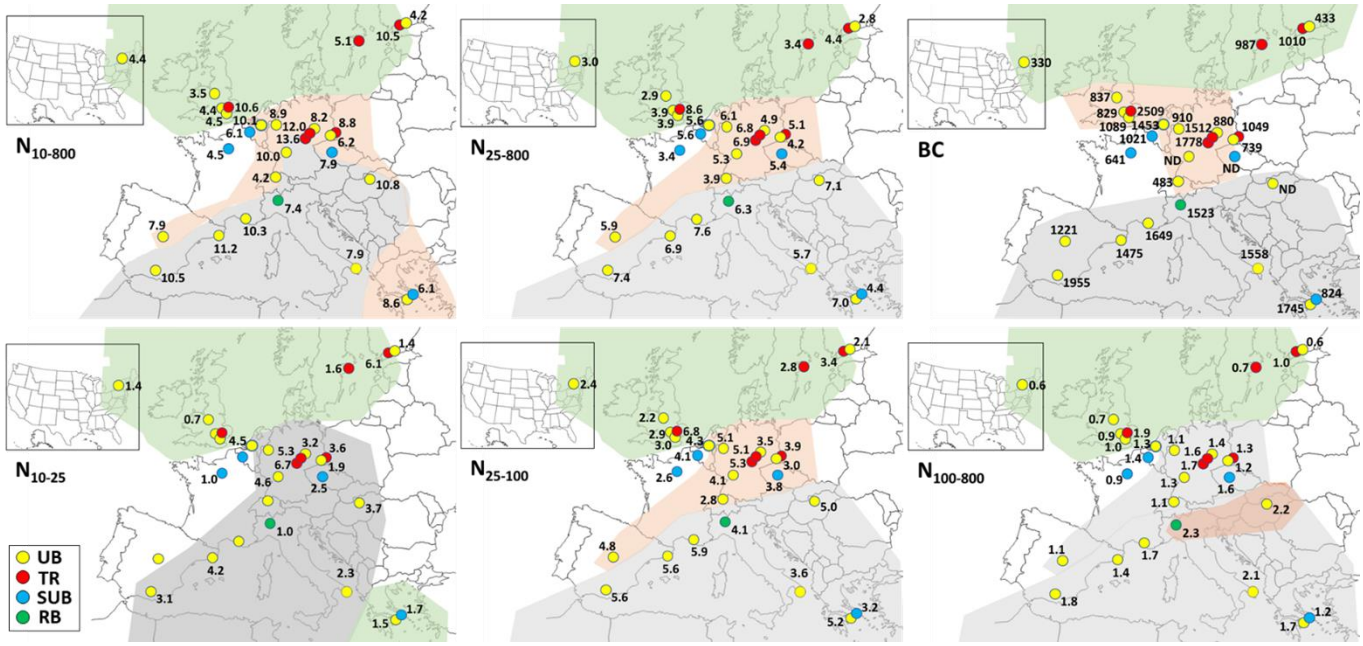


Figure 3: *Regional variability of averaged 2017-2019 particle number concentrations (in # cm^{-3} 10^{-3}) size fractions (in # cm^{-3} 10^{-3}) and black carbon (BC in ng m^{-3}) in Europe. For N_{10-25}, only sites with a lower size detection limit of 10-14 nm are included. UB, Urban background; TR, traffic; SUB, Suburban background; RB, Regional background. Modified from Trechera et al. (2023).*

Accumulation mode ($N_{100-800}$)

The Accumulation mode concentrations at the UB sites were also higher in southern Europe (1400-2200 # cm^{-3}, excluding MAD, 1100 # cm^{-3}) than in central (1100-1400 # cm^{-3}) and northern Europe, (600-1000 # cm^{-3}). Variability was high at the SUB and RB sites, with three SUB sites in the range 1200-1500 # cm^{-3}, PAR_SUB at 900 # cm^{-3} and ISP_RB at 2300 # cm^{-3}. Because the coarser detection limit varies across these datasets from 400 to 800 nm, it is difficult to make robust conclusions for this size mode.

4.3.4 Diel and seasonal patterns

Figures 4 and 5 show the diel patterns of BC, PNC (N_{10-800}), and N_{10-25}, N_{25-100} and $N_{100-800}$. When simultaneously evaluating daily and seasonal patterns of PNC and BC, the following three types of sites were differentiated:

Road traffic controlling ambient PNC (N_{10-800}): This type of site, of which ATH_UB is an example (see bottom of Figure 6), had a PNC peak at traffic rush hours and a PNC which was co-variant with BC (and NO_2, NO, NO_x and CO, not shown). Furthermore, the seasonal trends of BC and PNC were very similar, with high winter and low summer concentrations. At these sites, the midday PNC peak was very weak (or absent) compared with peaks during traffic rush hours. Thus, the daily BC and PNC trends were also very similar. In this case, the highest (but still very soft)

midday Nucleation mode occurred in winter-autumn, not in summer as in most cases. Furthermore, these sites were characterised by markedly lower weekend concentrations of both BC and PNC, pointing to a high impact of traffic emissions on the concentrations of both variables. The study sites with similar behaviour are GRA_UB, HEL_TR, LEC_UB, MAD_UB, MAR_UB, PAR_SUB, ROC_UB, STO_TR and ZUR_UB.

Conversely, some sites had **higher (than traffic rush hour) midday/morning PNC:** An example is LEI_UB (see top of Figure 6), in which the highest PNC was recorded outside traffic rush hours, at around 11-12 h. Hourly variations of averaged PNC were in parallel with O_3 and anti-correlated with BC. The midday PNC peak occurred (in summer, and also in spring and autumn with lower intensity) with very low BC concentrations. This can be attributed to regional or urban photo-nucleation and fumigation from higher atmospheric layers (enriched in Nucleation mode UFP and O_3 and depleted in BC, as the PBL grows by convective dynamics), and/or shipping and aviation and/or power plants and industry (see references above). In these cases, PNC maximised in summer and BC exhibited an opposite seasonal trend, with higher winter values. In most cases, weekend BC and UFP concentrations were lower. Sites included in this type are LEI_TR, LEI2_TR, DRE_UB, LAN_UB and PRA_SUB.

Intermediate type sites (different degrees of the prevalence of traffic/midday peaks and weak seasonal patterns): An example is BCN_UB (see middle of Figure 6). At this site, both traffic and midday peaks were present. Thus, PNC was parallel with BC except during the midday peak, but no seasonal patterns were noticeable, with similar PNC and BC all year. These sites also had high summer Nucleation mode peaks at midday, with lower intensities in spring and autumn. Weekend BC and PNC were markedly lower. These sites had weak seasonal patterns or no covariation of BC with PNC. However, some of these sites (BIR_UB, MUL_UB, HEL_UB, LIL_SUB, LND_UB, LND2_UB and LND_TR) had greater prevalence of traffic, with weak or no midday peaks and with traffic rush hour peaks. Other stations (ANT_UB, ATH_SUB, BUD, DRE_TR and ISP_RB) had greater prevalence of midday peaks, but did not exhibit the typical behaviour of high PNC and low BC values in summer.

This categorisation is similar to that found by Sun et al. (2019) for numerous sites in Germany.

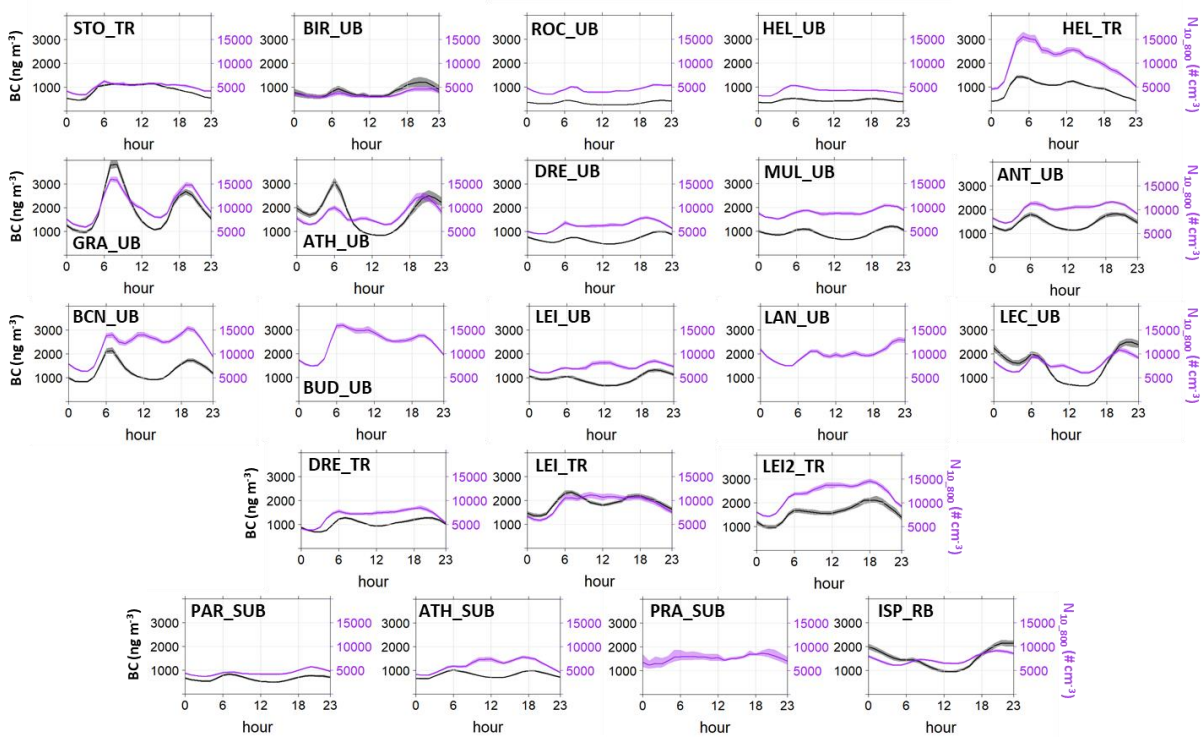


Figure 4: *Averaged 2017-2019 hourly concentrations of the particle number $N_{10\text{-}800}$ and black carbon (BC). Only sites with a lower size detection limit of 10-14 nm are included are considered. UB, Urban background; TR, Traffic; SUB, Suburban*

background; RB, Regional background. Particle number concentration units are # cm^{-3} 10^{-3} and those of BC in µg m^{-3}. Modified from Trechera et al. (2023).

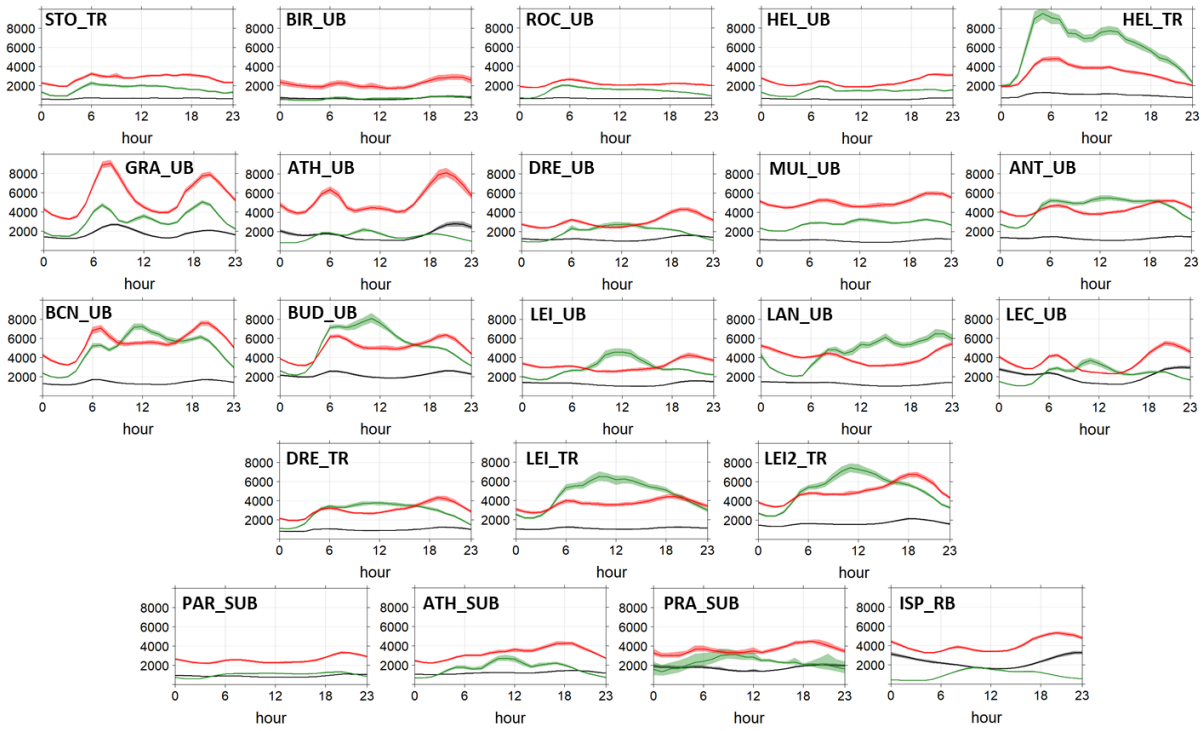


Figure 5: *Averaged 2017-2019 hourly concentrations of the particle number fractions (in # cm^{-3}) N_{10-25}, N_{25-100} and $N_{100-800}$. Only sites with a lower size detection limit of 10-14 nm are included. UB, Urban background; TR, Traffic; SUB, Suburban background; RB, Regional background. Modified from Trechera et al. (2023).*

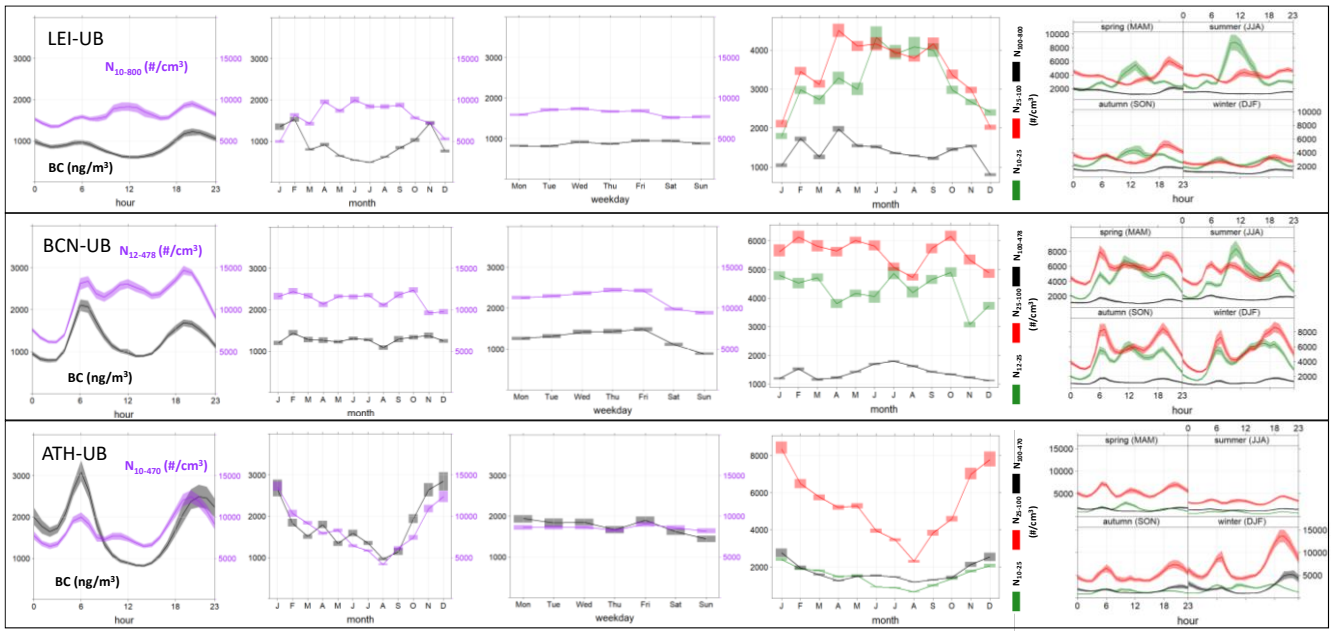


Figure 6: *Daily and seasonal patterns of UFP and BC for three Urban background stations in South Europe: LEI_UB, BCN_UB and ATH_UB. From Trechera et al. (2023).*

4.3.5 2009-2019 UFP-PNSD trends

Garcia-Marlès (2024a) evaluated long-term trends (5-11 years in 2009-2019) UFP/PNC concentrations and different particle size modes (UFP (N_{10-100}), PNC (N_{10-800}) and the Nucleation, Aitken and Accumulation modes (N_{10-25}, N_{25-100} and $N_{100-800}$, respectively)), based on PNSD measurements. Data from 21 sites (12 UB, 5 TR, 3 SUB and 1 RB) from 15 European and 1 US cities. Additionally, the trends in other pollutants and meteorological variables were evaluated in order to support interpretations.

UFP concentrations in urban Europe are largely influenced by road traffic emissions (Trechera et al., 2023, and references therein) as are other pollutants such as NO_X (i.e., NO and NO_2), CO, and BC. Concentrations of SO_2, BC, $PM_{2.5}$ and PM_{10} are influenced by other sources. In most cases European air quality policies resulted in marked reductions of emissions of these pollutants (EEA, 2023).

The results of this study show that in most studied European cities clear abatement of the BC, NO_2, PM, and the Aitken and Accumulation mode particle concentrations (Figure 7) followed the implementation of diesel particle filters (DPFs), from 2011 (EURO 5/V), and the subsequent abatement of NO_X emissions due to the controls required by EURO 6 and VI standards, which came into force in 2015, among other road traffic policies. Other air quality policy measures also generally produced SO_2 and CO decreases.

Reductions in urban NO_X emissions are expected to lead to an increase in O_3 due to a lesser titration by NO and to the reduction of NO_X concentrations in a VOCs-limited O_3 formation regime. This overall behaviour was observed at the majority of sites, especially at the traffic sites. Given the marked decrease in NO_2 and SO_2 concentrations, reduced nitrate and sulphate are also to be expected, and accordingly of PM.

The high influence of the road traffic emissions in the UFP, PNC, BC and NO_2 urban concentrations is also demonstrated by the higher declining slopes reached at the traffic (TR) sites compared to the urban background (UB) ones (Figure 8). Thus, these were 141, 57, 63 and 23% higher for the Aitken mode particles, Accumulation mode particles, BC and NO_2, respectively.

The trends in the Nucleation mode particles were far more diverse (statistically significant (ss) decreases at 6/21 sites and increases at 5/21 sites), with a non-ss increasing trend obtained for the UB sites (Figure 7). However, downward non-ss trends were obtained for the TR and SUB sites (Figure 7). The reduction of the Nucleation mode particles at TR sites was 50, 50, 11 and 93% lower than those obtained for Aitken and Accumulation mode particles (Figure 7), NO_X and BC, respectively. This is most probably due to inefficient removal of the semi-volatile diesel particle fraction by DPFs and a contribution from gasoline vehicles, expected to be predominantly in this size range, as previously reported by Chen et al. (2022) and Damayanti et al. (2023) for specific sites from US and Europe. These varying trends in the Nucleation mode particle number concentration are also affecting the UFP and total PNC trends, because of the high proportion of the Nucleation mode particles in both concentration ranges. Also, the 9-fold decrease of BC versus NO_X is probably result of the efficient impact of EURO 5 DPFs in abating ambient BC and the negative effect of the 'diesel gate' on ambient NO_X.

The diverse trends obtained for the Nucleation mode particles in UB sites might be due not only to the lack of emission controls for semi-volatile organic compounds escaping from DPFs, but also due to a reduction in condensation sink potential, which facilitates new particle formation. Moreover, at some sites, the presence of other substantial lower-mode UFP sources, such as photochemical nucleation, industry, shipping and aircraft emissions, also influence the trend of the Nucleation mode.

A generalized increase trend of temperature was also evidenced in most cities (Figure 9). This trend might have also influenced UFP trends, because on one way, it is known that temperature increases yield to lower UFP concentrations in urban areas and close to traffic sources (Weichenthal et al., 2008), and in another, increases of temperature and radiation might favour photochemical nucleation in urban areas (Brines et al., 2015).

Overall, the results presented here demonstrate the positive effects of the air quality policies implemented in Europe in abating air pollutants, including the Aitken and Accumulation mode particles, but less for the Nucleation

mode (Figure 7). The different modes of the PNSD should be evaluated independently to assess further policies promulgated to abate urban UFPs.

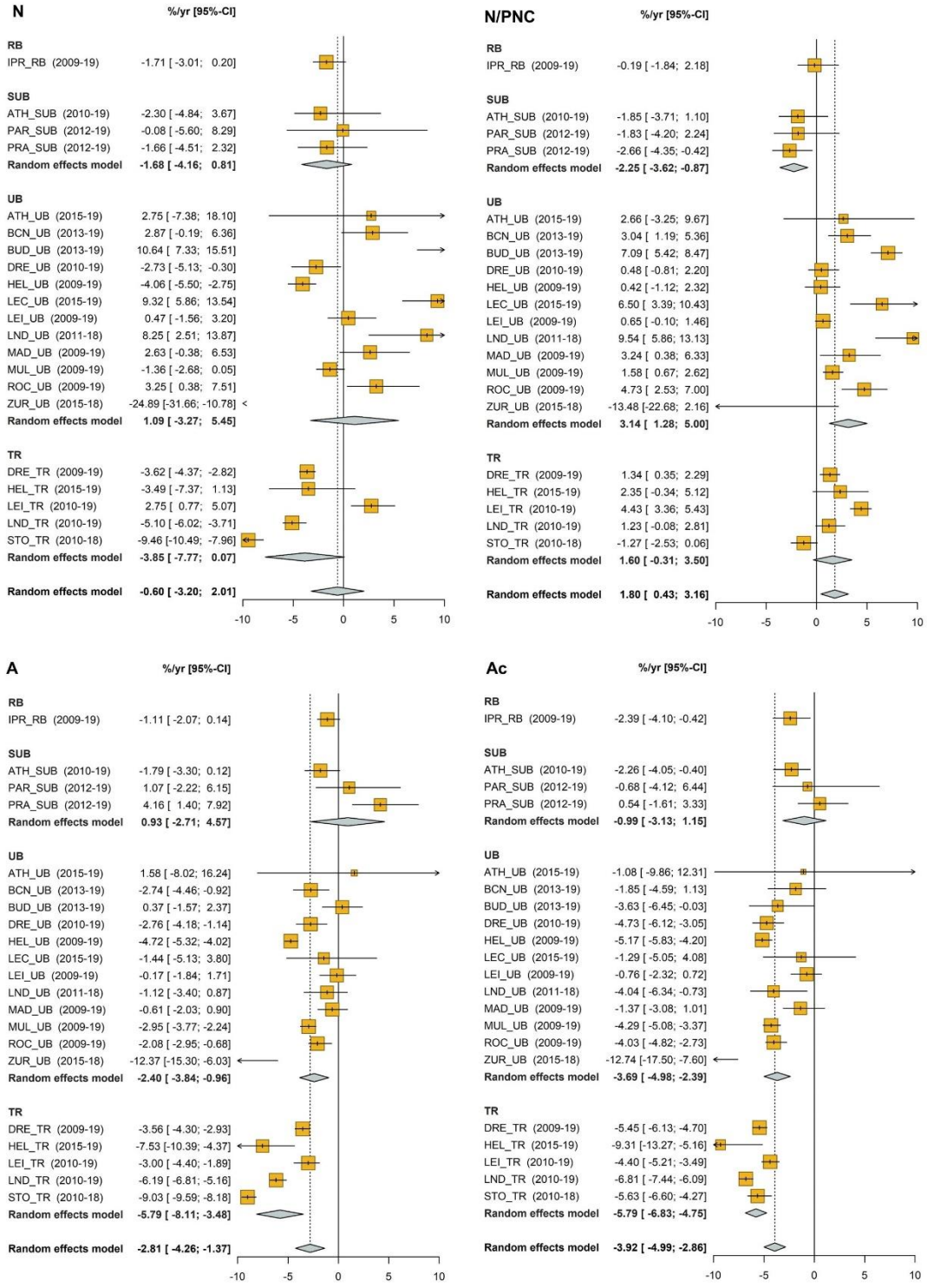


Figure 7: *Results of the trend analysis and subsequent meta-analysis for Nucleation mode (N), percentage of Nucleation mode particles in PNC (N/PNC), Aitken mode (A) and Accumulation mode (Ac) datasets. Trends are calculated using the Theil-Sen method. Results of the meta-analysis are presented globally for each pollutant and for the different site categories (UB, TR, SUB, and RB). The dashed lined represents the global meta-analysis. Random effects model: mean effect calculated for each type of site. From Garcia-Marlès et al (2024a).*

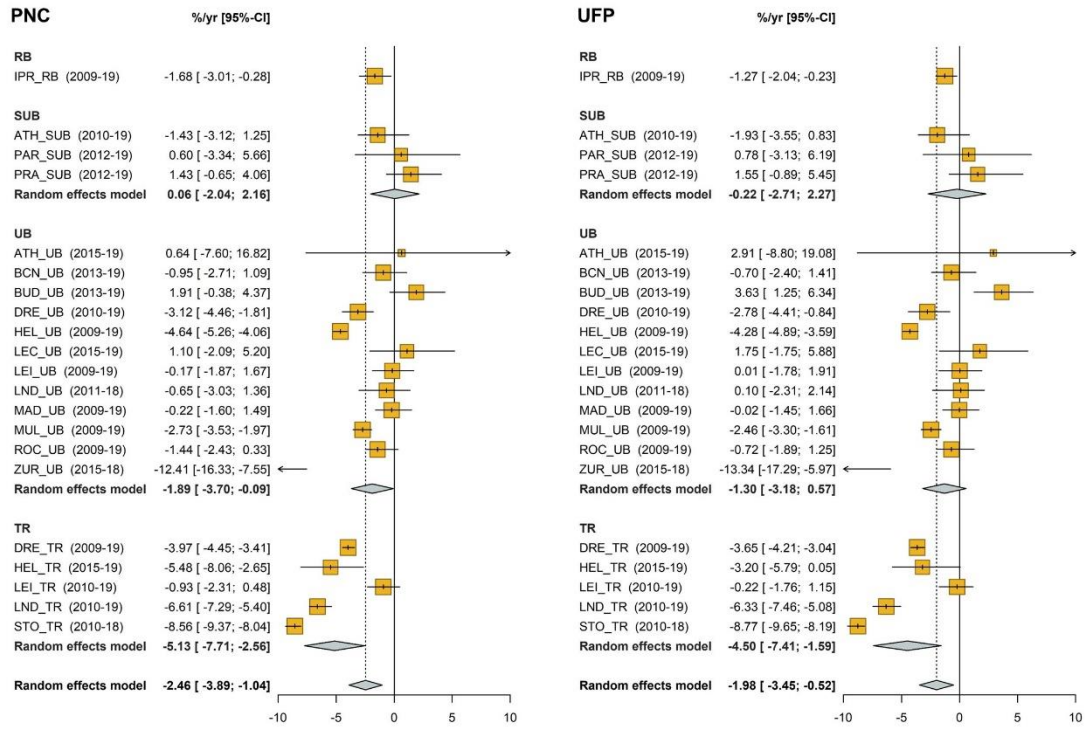


Figure 8: *Results of the trend analysis and subsequent meta-analysis for PNC and UFP datasets. Trends are calculated using the Theil-Sen method. Results of the meta-analysis are presented globally for each pollutant and for the different site categories (UB, TR, SUB, and RB). The dashed lined represents the global meta-analysis. Random effects model: mean effect calculated for each type of site. From Garcia-Marlès et al (2024a).*

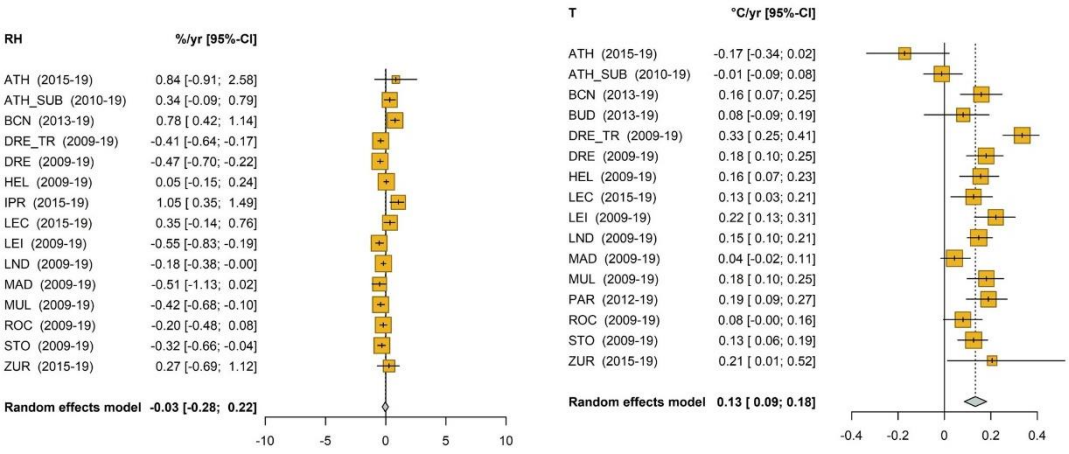


Figure 9: *Results of trend analysis and subsequent meta-analysis for relative humidity (RH, in % yr^{-1}) and Temperature (T, in ^{o}C yr^{-1}), with the slope and the 95% confidence intervals.*

4.4 Ambient air particulate total lung deposited surface area (LDSA) in urban Europe

Because of their small size, UFP might access deeper parts of the lungs, and even the bloodstream through lung translocation, thus causing systemic toxicity (Cassee et al., 2019). These UFPs also have a larger surface area for the

same mass than accumulation and coarse mode particles have. As a result, they can potentially carry more harmful substances into the alveoli and circulatory system, having a greater toxic effect than large diameter particles (Abdillah and Wang, 2022). Nowadays, a widely used approach to combine the lung deposition and surface area of particles is to measure or calculate the concentrations of lung deposited surface area (LDSA).

The determination of LDSA is of high interest for exposure assessment, as it reflects the concept that particle surface area available in the lung is a relevant exposure metric. LDSA has been proposed as a critical predictor for health outcomes from aerosol exposure, as it appears to be one of the most relevant physical metrics for evaluating exposure to particles (Chang et al., 2022). In prior studies, LDSA concentrations have been reported for ambient aerosols in different environments and several cities in the world but comparative data for total LDSA concentrations deposited in the all regions of lung for different site typologies (UB, TR, SUB, RB) are still very limited and needed.

In RI-URBANS, Liu et al. (2023) elaborated a study on the LDSA levels and variability in urban Europe, of which results are summarised below.

In UB sites, the highest annual average total LDSA concentration is found in BUD_UB (85 ± 53 $\mu m^2/cm^3$), followed by LEC_UB, GRA_UB and MAR_UB (72± 57, 63 ± 47, 63 ± 48 $\mu m^2/cm^3$), while the lowest is in ROC_UB (23 ± 15 $\mu m^2/cm^3$) and HEL_UB (24 ± 16 $\mu m^2/cm^3$). For TR site, the highest annual average total LDSA is found in LDN_TR (68 ± 41 $\mu m^2/cm^3$), followed by LEI2_TR (65 ± 39 $\mu m^2/cm^3$), while the lowest is in STO_TR (30 ± 16 $\mu m^2/cm^3$) and HEL_TR (39 ± 26 $\mu m^2/cm^3$). It is worth mentioning that data from TR sites from southern and eastern Europe were not available. For SUB areas, the highest annual average total LDSA is found in PRA_SUB (59 ± 81 $\mu m^2/cm^3$), followed by LIL_SUB (50 ± 34 $\mu m^2/cm^3$), while the lowest is in ATH_SUB (43 ± 24 $\mu m^2/cm^3$) and PAR_SUB (30 ± 22 $\mu m^2/cm^3$). Figure 10 (left) shows the European variability of LDSA levels.

The contributions of HA, TB, and ALV to total LDSA are summarized in Figure 10 (right). The results of the total LDSA concentration calculations show that LDSA is primarily accumulated in ALV (50%), which is considered to present the greatest potential health risk (Salo et al., 2021), and lower contributions were obtained for HA (16%) and TB (34%) deposition, consistent with the strong size-dependence of deposition (Kumar et al., 2014). A previous study reporting an estimation for the inhaled deposited dose rate during common exposure scenarios for UB aerosols in Amman, Jordan, reported HA, TB, and ALV inhaled deposited doses reaching 7-16%, 16-28%, and 56-76%, respectively (Hussein et al., 2022). In comparison, a prior study in the Helsinki metropolitan area found that the annual mean ALV-LDSA concentrations varied between 9 and 22 $\mu m^2/cm^3$ at different sites (Kuula et al., 2020). The range was 9-12 $\mu m^2/cm^3$ for urban background and detached housing area sites, which are quite clean areas in Helsinki (Kuula et al., 2020), to values up to ~189 $\mu m^2/cm^3$ typically observed near PM sources such as urban roads in Athens, Greece (Cheristanidis et al., 2020). This range was confirmed by our results where the ALV-LDSA annual averages range from 12 ± 8 to 41 ± 29 $\mu m^2/cm^3$, pointing to a significant heterogeneity of LDSA across urban Europe.

Diel of total LDSA show similar patterns among all monitoring sites (not shown). At the UB sites, a morning LDSA peak coincides with traffic rush hours. A prior study also reported that during rush hour, about 74% of LDSA is attributed to traffic emitted particles (Chang et al., 2022). Furthermore, it is also worth noting that the morning peak of LDSA at TR sites starts earlier (4:30-6:00 UTC), is more pronounced, remains high until the evening traffic peak (~19:00 UTC), and then slightly decreases, further illustrating the impact of traffic on total LDSA (Reche et al., 2015).

The weekly average variations of the total LDSA concentrations at UB and TR sites (not shown) are characterized by higher workday values.

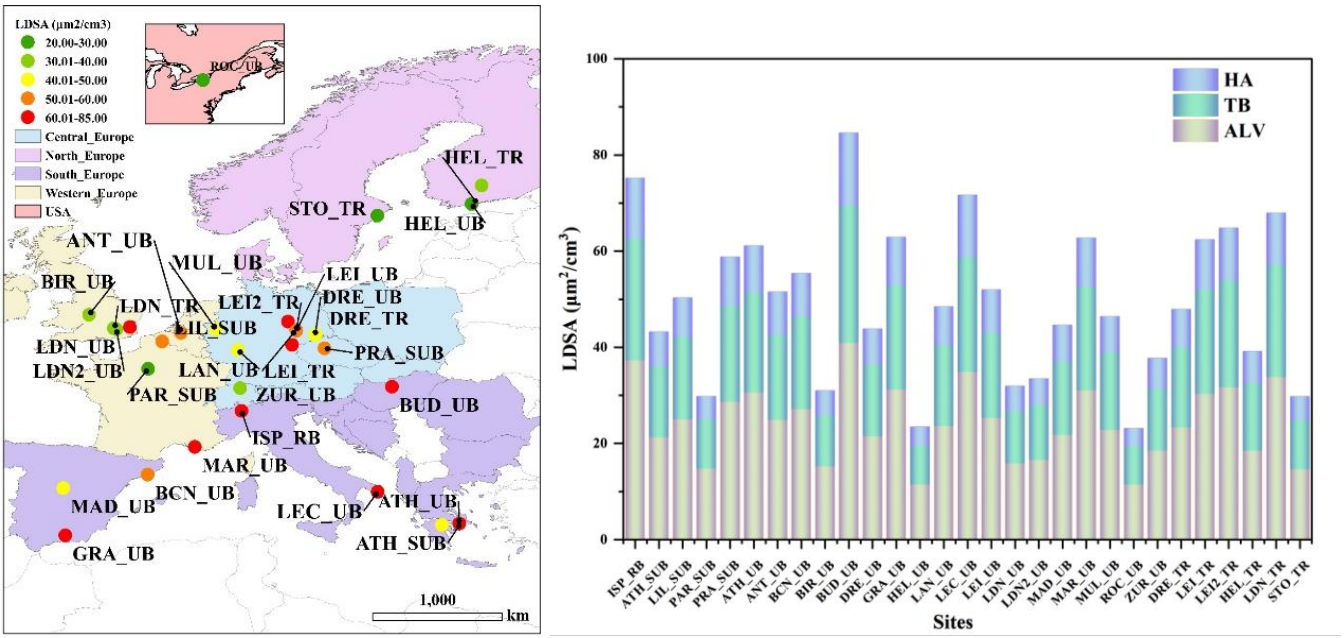


Figure 10: *Left: 2017-2019 average concentrations (μm²/cm³) of total LDSA at 29 European sites and one from the USA; urban background (UB), suburban background (SUB), regional background (RB) and traffic (TR) sites (modified from Liu et al., 2023). Right: Contributions (in %) to total LDSA of those from head/throat (HA), tracheobronchial (TB), and alveolar (ALV) regions.*

By season (Figure 11), total LDSA concentrations show substantial seasonal differences in a number of cities, but not in other. In winter, the highest average exposures to LDSA metrics are found at ATH_UB, BUD_UB, GRA_UB, LEC_UB, LDN2_UB, MAD_UB, ZUR_UB, DRE_TR, ISP_RB, PAR_SUB, and PRA_SUB. The increase in total LDSA concentration in winter may be influenced by the emissions from residential heating, traffic emissions, and meteorological conditions favouring stagnation. During summer, sites such as BCN_UB, HEL_UB, LAN_UB, LDN_UB, ROC_UB, LIL_SUB, HEL_TR, and STO_TR have the highest average total LDSA, while during spring, DRE_UB, LEI_UB, LEI_TR, LEI2_TR, and LDN_TR have the highest average total LDSA. Previous research by (Masiol et al., 2018) found Accumulation mode PNC peaked at the ROC_UB site in summer due to increased photochemical activity leading to more secondary particle formation, this phenomenon was also observed in Germany (e.g., Dresden, Berlin, etc.) (Junkermann et al., 2016). In addition, in Helsinki, Finland (e.g., HEL_UB, HEL_TR), it may be due to long-range atmospheric transport and vertical downward transport from high altitude atmospheric layers enriched in Nucleation and Aitken mode particles (Lampilahti et al., 2021). Finally, in Barcelona (BCN_UB), factors such as agricultural burning and forest fires, shipping, and aviation may contribute to high total LDSA in summer (Rivas et al., 2020).

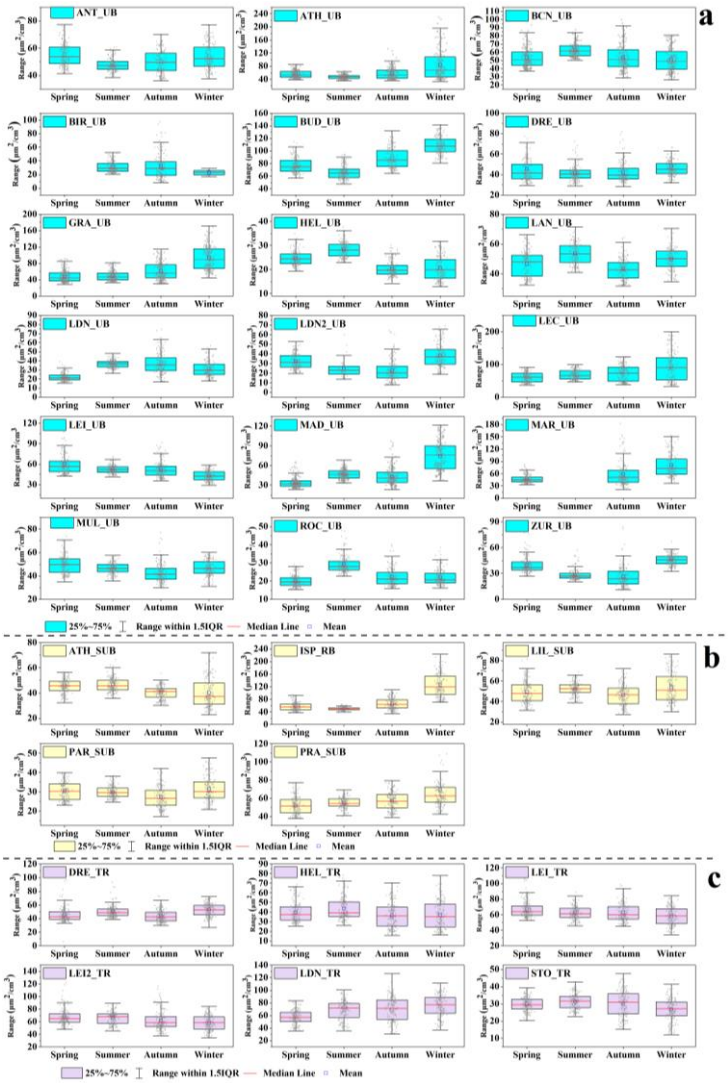


Figure 11: *2017-2019 seasonal variations of total LDSA concentrations for 27 out of the 29 studied sites. a, urban background (UB) sites; b, suburban background (SUB) and regional background (ISP_RB) sites; and c, traffic (TR) sites (modified from Liu et al., 2023).*

5. RECOMMENDATIONS AND MAIN FINDINGS

5.1 Recommendations on measurements, quality control and data management

Data compilation from 29 urban sites carried out in RI-URBANS demonstrated the need of increasing particle number concentration (PNC) and particle number size distribution (PNSD) measurements in urban areas in Europe, mainly in Eastern and Southern Europe. Measurements are not comparable due to the lack of harmonized protocols and, specifically, due to the different lower sizes measured.

5.1.1 Sampling system

Sampling systems and requirements are detailed described in the CEN standards. Sampling lines should be as short as possible and made of conductive material in order to minimize the loss of particles by diffusion. Particle losses due to diffusion: have to be determined and corrected for, based on equivalent lengths. On the other hand, there is an inconsistency between the air quality requirements (2008/50/CE) and the CEN standards in the height of the sampling inlet. While the first, request 1.5 to 4 m above the ground, and exceptionally up to 8 m, the CEN standards suggest 5 to 10 m to measure undisturbed atmospheric aerosol. Another inconsistency was found on the basis of the concentrations of aerosol particles. While the first request ambient conditions for the concentrations of PM, the CEN standards request STP conditions for PNC and PNSD measurements.

The in-situ aerosol measurements should be done at a relative humidity lower than 40%. This is necessary to obtain comparable data, independent of the hygroscopic growth. Nafion or membrane dryers are recommended for reducing humidity of the aerosol sample minimizing the interferences in the measurement. This may require the use of extra pumps and/or compressors for supplying dry air and, consequently, it requires additional cabinet/container space.

5.1.2 Particle size range

The “new” prEN 16976:2023 for the “Determination of the particle number concentration of atmospheric aerosol” describes a standard method for determining the particle number concentration based on a CPC and sets 10 nm as the lower limit of the measured particle size range.

The CEN/TS 17434:2020 for “Determination of the particle number size distribution of atmospheric aerosol using a Mobility Particle Size Spectrometer (MPSS)” describes a standard method for determining the particle number size distribution in ambient air in the size range from 10 to 800 nm.

Thus, the lower limit of the measured size range is identical for both measurements, favouring the comparison of the measurements for the PNC performed in Europe. Moreover, measuring in parallel by collocating an MPSS CEN/TS 17434:2020) and a CPC (prEN 16976:202) permits to check the accuracy of the integrated number concentration measurement by the MPSS.

Setting 10 nm as a lower limit hampers the measurement of the nucleation mode, accounting for an important fraction of PNC. Measuring PNC <10nm can be of capital interest in areas with intense photo-nucleation (e.g. Mediterranean countries with high insolation) or in hotspots. It is worthy to comment that the proposed EU AQ Directive establish the need of measuring UFP in supersites but also close to hotspots (e.g. road sites, harbours, airports…). For these reasons, RI-URBANS recommend to install a nano-CPC (measuring PNC >3nm or PNC >1nm) in parallel to the standard CPC and MPSS.

5.1.3 Instrument performance

ACTRIS provides results of performance test for different CPC and MPSS models validating the CEN or ACTRIS compliance (ACTRIS 2024b). External calibrations are very important in addition to the frequent maintenance.

Both CEN standards describe in detail the requirements of the instruments to be used for PNC and PNSD measurements. Nowadays, there is a number of commercial CPC and MPSS instruments available complying with CEN standards

For CPCs, the use of n-butanol as vapor substance is mandatory and may be an issue for installation in monitoring networks where technicians from different companies may access. Accessories for removing ambient butanol into the monitoring stations area available, but this will generate extra costs.

Use of bipolar diffusion chargers is required for MPSS. Radioactive sources (^{85}Kr, ^{63}Ni, ^{241}Am and ^{210}Po) are recommended. These may require a radioactive license and can be an issue in some countries. Soft X-ray source can also be used (not license needed) but must use a model-specific bipolar charge distribution if available. Moreover, live time of the soft X-ray source is rather short, and they shall be frequently renovated, considerably increasing the operation costs.

5.1.4 Maintenance and quality control

Maintenance and operation are key issues: operation and quality control are well described in CEN standards. However, these techniques are complex and require specialized technicians. Thus, RI-URBANS corroborated very low data coverage (<70%) for most of the sites, from which the data were compiled. Specific training is needed for operators of companies that maintain AQ monitoring networks. In any case, a >90% coverage time (excluding the maintenance periods) is recommended.

5.1.5 Calibration infrastructures

As done for conventional AQ measurements in Europe, it is suggested that the National reference AQ Laboratories send CPC and MPSS instruments to a calibration centre (such as the CAIS-ECAC ACTRIS Topical Centre) and then carry out secondary calibrations of national instruments in their laboratories. However, instrumental setups of calibration facilities for CPC and MPSS are expensive and required skilled personal.

5.1.6 Data management

The corresponding CEN standards recommend to follow the EBAS protocols for data reporting and data management. These protocols were stablished by EBAS in collaboration with EUSAAR and ACTRIS infrastructure.

EBAS defined 3 data levels and corresponding data file formats: Level 0, Level 1, and Level 2. Data, metadata and flags to be reported for each Level are indicated in prEN 16976:2023 and CEN/TS 17434:2020.

Level 2 data contains hourly averages and concentration stated for standard temperature and pressure conditions (273.15 K; 1013.25 hPa). It is worthy to note that in AQ standards concentrations of particulate pollutants are reported at ambient conditions. This inconsistency shall be solved if EBAS is compiling data for AQ users.

5.2 Main findings for PNC-PNSD in urban Europe

5.2.1 Instrument and data management

- Only 18/29 datasets reached >70% of data availability, reflecting the complexity of PNC-PNSD measurements, which require detailed monitoring and constant maintenance of the instrumentation.
- The lack of harmonisation of PNSD measurement accounts for significant differences of the lower size detection limits (3 to 20 nm), which makes the direct comparison of ultrafine particles (UFP) and PNC concentrations from different sites difficult, especially those in the Nucleation mode (<25 nm). To increase comparability, an effort should be made to implement the CEN and ACTRIS recommendations. There was also often a lack of frequent quality assurances in the past leading to enhanced uncertainties not only for the range below 20 nm.
- Only 12/29 datasets are openly available in the EBAS data infrastructure, and accordingly, an effort should also direct at making data open for use in air quality health research and policy support.

5.2.2 Concentrations of UFP-PNSD

- UFP-PNC urban concentrations follow a clear increasing trend from northern to southern and eastern Europe, and an even more marked trend for N_{25-100} and N_{25-800}. These trends are similar to those found for BC.
- PNCs follow the TR>UB>SUB trend. However, PNC in the RB of the Po Valley are equivalent to those of an UB in southern Europe.
- The major contributing source to PNC in urban Europe is road traffic as deduced from the parallel daily patterns to those of BC, with peak concentrations at traffic rush hours.
- However, a relevant number of sites recorded high PNCs (in some cases exceeding those of traffic) in the morning-midday coinciding with minimal BC, and the highest temperature, wind speed, insolation and O_3. These marked morning-midday maxima are caused by pronounced increases of N_{10-25} (Nucleation mode).
- The highest midday PNC-Nucleation modes are recorded in central Europe followed by southern Europe, so these do not follow only insolation as it should be expected from new particle formation from regional photochemical nucleation. Thus, the origin of these midday marked maxima are attributed to photochemical nucleation, surface fumigation of high-altitude atmospheric layers transporting high SO_2 plumes and plumes from airports, shipping, or power or industrial plants. In a relevant proportion of the study sites, the contribution of these sources/processes to the annual PNC is very significant.
- Daily and seasonal patterns are used to classify the PNSD datasets in three major groups: i) low midday PNC peaks and PNC parallel daily patterns, with high winter BC and PNC, with low spring-summer $_{N10-25}$; ii) PNC and BC traffic-related daily patterns, but a major midday PNC peak with low BC concentrations, with inverse seasonal PNC (highest in spring-summer) and BC (highest in autumn-winter) patterns, with very intensive N_{10-25} midday peaks in spring and summer; and iii) as type ii, but with dominant traffic-related PNC peaks, but marked midday N_{10-25} peaks and no definite seasonal patterns.

5.2.3 UFP-PNSD 2009-2019 concentration trends

- UFP concentrations in urban Europe are largely influenced by road traffic emissions, as are other pollutants such as NO_X (i.e., NO and NO_2), CO, and BC. Concentrations of SO_2, BC, $PM_{2.5}$ and PM_{10} are influenced by other sources. In most cases European air quality policies resulted in marked reductions of emissions of these pollutants (EEA, 2023).
- In most studied European cities clear abatement of the BC, NO_2, PM, and the Aitken and Accumulation mode particle concentrations followed the implementation of diesel particle filters (DPFs), from 2011 (EURO 5/V), and the subsequent abatement of NO_X emissions due to the controls required by EURO 6 and VI standards, which came into force in 2015, among other road traffic policies. Other air quality policy measures also generally produced SO_2 and CO decreases.
- The high influence of the road traffic emissions in the UFP, PNC, BC and NO_2 urban concentrations is also demonstrated by the higher declining slopes reached at the traffic (TR) sites compared to the urban background (UB) ones.
- The trends in the Nucleation mode particles were far more diverse (ss decreases at 6/21 sites and increases at 5/21 sites), with a non-ss increasing trend obtained for the UB sites. However, downward non-ss trends were obtained for the TR and SUB sites. The reduction of the Nucleation mode particles at TR sites was much lower than those obtained for Aitken and Accumulation mode particles, NO_X and BC. This is most probably due to inefficient removal of the semi-volatile diesel particle fraction by DPFs and a contribution from gasoline vehicles, expected to be predominantly in this size range, as previously reported by Chen et al. (2022) and Damayanti et al. (2023) for specific sites from US and Europe. These varying trends in the Nucleation mode particle number concentration are also affecting the UFP and total PNC trends, because of the high proportion of the Nucleation mode particles in both concentration ranges.
- The diverse trends obtained for the Nucleation mode particles in UB sites might be due not only to the lack of emission controls for semi-volatile organic compounds escaping from DPFs, but also due to a reduction in condensation sink potential, which facilitates new particle formation. Moreover, at some sites, the presence of

other substantial lower-mode UFP sources, such as photochemical nucleation, industry, shipping and aircraft emissions, also influence the trend of the Nucleation mode.

- A generalized increase trend of temperature was also evidenced in most cities. This trend might have also influenced UFP trends, because on one way it is known that temperature increases yield to lower UFP concentrations in urban areas and close to traffic sources (Weichenthal et al. (2008), and in another the temperature and radiation increases might favour photochemical nucleation in urban areas (Brines et al., 2015).
- Overall, the results presented here demonstrate the positive effects of the air quality policies implemented in Europe in abating air pollutants, including the Aitken and Accumulation mode particles, but less for the Nucleation mode. The different modes of the PNSD should be evaluated independently to assess further policies promulgated to abate urban UFPs.

5.2.4 Levels of aerosol Lung Deposited Surface Area (LDSA) in urban Europe

- LDSA levels can be obtained from PNSD measurements.
- The annual range of concentration for all sites is between 20-85 $\mu m^2/cm^3$.
- There are lower UB concentrations in Northern Europe and higher concentrations in Southern Europe, with a trend of TR> UB > SUB.
- LDSA shows significant differences in concentrations and time variability among different regions and types of sites, which may be caused by the changes in the sources of UFP and larger particles, emission rates, traffic volume, and meteorological factors, including those favouring new particle formation, stagnation, long-range transport, vertical transport of aerosols, and influence from plumes from pollution hotspots.
- Correlations of total LDSA with other pollutant metrics show that PNC in the Aitken and Accumulation modes are mainly associated with the total LDSA concentration.
- The results also indicated that the main proportion of LDSA is attributed to the ALV (50% on average at all sites), followed by the TB (34%) and HA (16%) fractions.

6. REFERENCES

Abdillah, S.F., Wang, Y., 2022. Ambient ultrafine particle (PM0.1): sources, characteristics, measurements and exposure implications on human health. Environ. Res., 115061.

ACTRIS, 2024a. Recommendations, guidelines, standard operating procedures and scientific articles for aerosol in-situ measurements: particle number concentration >10 nm, https://www.actris-ecac.eu/pnc-greater-10nm.html

ACTRIS, 2024b. Recommendations, guidelines, standard operating procedures and scientific articles for aerosol in-situ measurements: particle number size distribution – mobility diameter 10 to 80 nm. https://www.actris-ecac.eu/pnsd-10-to-800nm.html

ACTRIS 2024c. ACTRIS-ERIC Aerosols in-situ Instruments Compliance. https://www.actris-ecac.eu/actris-gaw-recommendation-documents.html

Balduzzi, S., Rücker, G., Schwarzer, G., 2019. How to perform a meta-analysis with R: a practical tutorial. Evidence-Based Mental Health, 22, 153–160, https://doi.org/10.1136/ebmental-2019-300117

Brines, M., Dall'Osto, M., Beddows, D.C.S., Harrison, R.M., Gómez-Moreno, F., Núñez, L., Artíñano, B., Costabile, F., Gobbi, G.P., Salimi, F., Morawska, L., Sioutas, C., Querol, X., 2015. Traffic and nucleation events as main sources of ultrafine particles in high-insolation developed world cities. Atmos. Chem. Phys., 15, 5929–5945, https://doi.org/10.5194/acp-15-5929-2015

Carslaw, D.C. and Ropkins, K., 2012. Openair - an R package for air quality data analysis. Environ. Model. Software, 27, 28, 52–61, https://doi.org/10.1016/j.envsoft.2011.09.008

Cassee, F.R., Morawska, L., Peters, A., 2019. ambient ultrafine particles: evidence for policy makers. Thinking Outside the Box Report.

CEN/TS 17434:2020 "Ambient air - Determination of the particle number size distribution of atmospheric aerosol using a Mobility Particle Size Spectrometer (MPSS)". Technical Committee CEN/TC 264 "Air Quality".

Chang, P., Griffith, S.M., Chuang, H., Chuang, K., Wang, Y., Chang, K., Hsiao, T., 2022. Particulate matter in a motorcycle-dominated urban area: source apportionment and cancer risk of lung deposited surface area (ldsa) concentrations. J. Hazard. Mater., 427, 128188, https://doi.org/10.1016/j.jhazmat.2021.128188.

Chen, D.G.D. and Peace, K.E., 2013. Applied meta-analysis with R. CRC press.

Chen, Y., Masiol, M., Squizzato, S., Chalupa, D.C., Zíková, N., Pokorná, P., Rich, D.Q., Hopke, P.K., 2022. Long-term trends of ultrafine and fine particle number concentrations in New York State: Apportioning between emissions and dispersion. Environ. Poll., 310, 119797, https://doi.org/10.1016/j.envpol.2022.119797

Damayanti S., Harrison R.M., Pope F., Beddows D.C.S., 2023. Limited impact of diesel particle filters on road traffic emissions of ultrafine particles. Environ. Int., 174, 107888, https://doi.org/10.1016/j.envint.2023.107888

Cheristanidis, S., Grivas, G., Chaloulakou, A., 2020. Determination of total and lung-deposited particle surface area concentrations, in central athens, greece. Environ. Monit Assess., 192 10, 627, https://coi.org/10.1007/s10661-020-08569-8.

Diesch, J.M., Drewnick, F., Klimach, T., Borrmann, S., 2013. Investigation of gaseous and particulate emissions from various marine vessel types measured on the banks of the Elbe in Northern Germany. Atmos. Chem. Phys., 13, 3603–3618, https://doi.org/10.5194/acp-13-3603-2013

Garcia-Marlès, M., Lara, R., Reche, C., Pérez, N, Tobías, A., Savadkoohi, M., Beddows, D., et al., 2024a. Inter-annual trends of ultrafine particles in urban Europe. Environ. Int., 185, 108510,> https://doi.org/10.1016/j.envint.2024.108510

Garcia-Marlès, M., Lara, R., Reche, C., Pérez, N, Tobías, A., Savadkoohi, M., Beddows, D., et al., 2024b. Source apportionment of ultrafine particles in urban Europe. Environ. Int. (Sumitted).

GAW/WMO Aerosol Measurement Procedures, Guidelines and Recommendations, 2016. GAW Report N. 227, WMO-No. 1177, https://library.wmo.int/records/item/55277-wmo-gaw-aerosol-measurement-procedures-guidelines-and-recommendations?offset=89

Harrison, R.M., Beddows, D.C.S., Dall'Osto, M., 2011. PMF analysis of wide-range particle size spectra collected on a major highway. Environ. Sci. Technol., 45, 5522–5528, https://doi.org/10.1021/es2006622

Hopke, P.K., Feng, Y., Dai, Q., 2022. Source apportionment of particle number concentrations: A global review. Sci. Total Environ., 819, 153104, https://doi.org/10.1016/j.scitotenv.2022.153104

Hopke, P.K., Chen, Y., Chalupa, D.C., Rich, D.Q., 2024. Long term trends in source apportion particle number concentrations in Rochester NY. Environ. Pollut. 347, 123708. https://doi.org/10.1016/j.envpol.2024.123708

Hussein, T., Al-Abdallat, A., Saleh, S.S.A., Al-Kloub, M., 2022. Estimation of the seasonal inhaled deposited dose of particulate matter in the respiratory system of urban individuals living in an eastern Mediterranean city. Int. J. Environ. Res. Pub. Health 19, 7, 4303, https://doi.org/10.3390/ijerph19074303

Junkermann, W., Vogel, B., Bangert, M., 2016. Ultrafine particles over Germany: an aerial survey. Tellus B: Chem. Phys. Meteo., 68, 1, 29250, https://doi.org/10.3402/tellusb.v68.29250

Kumar, P., Morawska, L., Birmili, W., Paasonen, P., Hu, M., Kulmala, M., et al., 2014. Ultrafine particles in cities. Environ. Int. 66, 1-10, https://doi.org/10.1016/j.envint.2014.01.013

Kuula, J., Kuuluvainen, H., Niemi, J.V., Saukko, E., Portin, H., Kousa, A., Aurela, M., et al., 2019. Long-term sensor measurements of lung deposited surface area of particulate matter emitted from local vehicular and residential wood combustion sources. Aerosol. Sci. Technol., 54 2, 190-202, https://doi.org/10.1080/02786826.2019.1668909.

Lampilahti, J., Leino, K., Manninen, A., Poutanen, P., Franck, A., Peltola, M., Hietala, P., et al., 2021. Aerosol particle formation in the upper residual layer. Atmos. Chem. Phys., 21, 10, 7901-7915, https://doi.org/10.5194/acp-21-7901-2021

Liu, X., Hadiatullah. H., Zhang. X., Trechera. P., Savadkoohi. M., Garcia-Marlès, M., et al., 2023. Ambient air particulate total lung deposited surface area (LDSA) levels in urban Europe,Ambient air particulate total lung deposited surface area (LDSA) levels in urban Europe. Sci. Total Environ. 898, 165466, https://doi.org/10.1016/j.scitotenv.2023.165466

Lorentz, H., Janicke, U., Jakobs, H., Schmidt, W., Hellebrandt, P., Ketzel, M., Gerwig, H., 2019. Ultrafine particle dispersion modelling at and around Frankfurt airport (FRA), Germany. 19th International Conference on Harmonisation within Atmospheric Dispersion Modelling for Regulatory Purposes. 3-6 June 2019, Bruges, Belgium, H19-082, https://www.harmo.org/Conferences/Proceedings/_Bruges/publishedSections/H19-082%20Helmut%20Lorentz.pdf

Masiol, M., Squizzato, S., Chalupa, D.C., Utell, M.J., Rich, D.Q., Hopke, P.K., 2018. Long-term trends in submicron particle concentrations in a metropolitan area of the north-eastern United States. Sci. Total Environ., 633, 59-70, https://doi.org/10.1016/j.scitotenv.2018.03.151

Norris, G., Duvall, R., Brown, S., Song, B., 2014. EPA positive matrix factorization (PMF) 5.0 fundamentals and user guide, https://www.epa.gov/air-research/epa-positive-matrix-factorization-50-fundamentals-and-user-guide

prEN 16976: "Ambient air - Determination of the particle number concentration of atmospheric aerosol". Currently being prepared by the Technical Committee CEN/TC 264 "Air Quality" (Draft).

Putaud, J.P., Pozzoli, L., Pisoni, E., Martins Dos Santos, S., Lagler, F., Lanzani, G., Dal Santo, U., Colette, A., 2021. Impacts of the COVID-19 lockdown on air pollution at regional and urban background sites in northern Italy. Atmos. Chem. Phys. 21, 7597–7609, https://doi.org/10.5194/acp-21-7597-2021

Reche, C., Viana, M., Brines, M., Pérez, N., Beddows, D., Alastuey, A., Querol, X., 2015. Determinants of aerosol lung-deposited surface area variation in an urban environment. Sci Total Environ 517, 38-47, https://coi.org/https://doi.org/10.1016/j.scitotenv.2015.02.049.

Reddy, B.S.K., Kumar, K.R., Balakrishnaiah, G., Gopal, K.R., Reddy, R.R., Reddy, L., et al., 2012. Potential source regions contributing to seasonal variations of black carbon aerosols over Anantapur in southeast India. Aerosol Air. Qual. Res. 12, 3, 344-358, https://doi.org/10.4209/aaqr.2011.10.0159

Rivas, I., Beddows, D.C., Amato, F., Green, D.C., Järvi, L., Hueglin, C., Reche, C., et al., 2020. Source apportionment of particle number size distribution in urban background and traffic stations in four European cities. Environ. Int., 135, 105345, https://doi.org/10.1016/j.envint.2019.105345

Rivas, I., Vicens, L., Basagaña, X., Tobías, A., Katsouyanni, K., Walton, H., Hüglin, C., Alastuey, A., et al., 2021. Associations between sources of particle number and mortality in four European cities. Environ. Int., 155, https://doi.org/10.1016/j.envint.2021.106662

Salo, L., Hyvärinen, A., Jalava, P., Teinilä, K., Hooda, R.K., Datta, A., Saarikoski, S., et al., 2021. The characteristics and size of lung-depositing particles vary significantly between high and low pollution traffic environments. Atmos. Environ., 255, 118421, https://doi.org/10.1016/j.atmosenv.2021.118421

Salo, L., Rönkkö, T., Saarikoski, S., Teinilä, K., Kuula, J., Alanen, J., Arffman, A., Timonen, H., Keskinen, J., 2021. Concentrations and size distributions of particle lung-deposited surface area (ldsa) in an underground mine. Aerosol Air. Qual. Res., 21, 8, 200660, https://doi.org/10.4209/aaqr.200660

Sen, P.K., 1968. Estimates of the regression coefficient based on Kendall's Tau. J. Am. Stat. Assoc. 63, 1379–1389.

Stacey B., Harrison R.M., Pope F., 2020. Evaluation of ultrafine particle concentrations and size distributions at London Heathrow Airport. Atmos. Environ., 222, 117148, https://doi.org/10.1016/j.atmosenv.2019.117148

Sun, J., Birmili, W., Hermann, M., Tuch, T., Weinhold, K., Spindler, G., Schladitz, A., Bastian, Set al., 2019. Variability of black carbon mass concentrations, sub-micrometer particle number concentrations and size distributions: results of the German Ultrafine Aerosol Network ranging from city street to High Alpine locations. Atmos. Environ., 202, 256–268, https://doi.org/10.1016/j.atmosenv.2018.12.029

Theil, H., 1992. A rank-invariant method of linear and polynomial regression analysis. In: Raj, B., Koerts, J. (Eds.), Henri Theil's Contributions to Economics and Econometrics, Advanced Studies in Theoretical and Applied Econometrics, 23. Springer, Dordrecht, https://doi.org/10.1007/978-94-011-2546-8_20

Torkmahalleh, M.A., Akhmetvaliyeva, Z., Omran, A.D., Darvish Omran, F., Kazemitabar, M., et al., 2021. Global Air Quality and COVID-19 Pandemic: Do We Breathe Cleaner Air? Aerosol Air Qual. Res., 21, 200567, https://doi.org/10.4209/aaqr.200567

Trechera, P., Garcia-Marlès, M., Liu, X., Reche, C., Pérez, N., Savadkoohi, et al., 2023. Phenomenology of ultrafine particle concentrations and size distribution across urban Europe. Environ. Int., 172, 107744, https://doi.org/10.1016/j.envint.2023.107744

Vörösmarty, M., Hopke, P. K., Salma, I., 2024. Attribution of aerosol particle number size distributions to main sources using an 11-year urban dataset, Atmos. Chem. Phys., 24, 5695–5712. https://doi.org/10.5194/acp-24-5695-2024.

Vratolis, S., Gini, M.I., Bezantakos, S., Stavroulas, I., Kalivitis, N., Kostenidou, E., Louvaris, E., et al., 2019. Particle number size distribution statistics at City-Centre Urban Background, urban background, and remote stations in Greece during summer. Atmos. Environ., 213, 11-726, https://doi.org/10.1016/j.atmosenv.2019.05.064

Weichenthal, S., Dufresne, A., Infante-Rivard, C. et al., 2008. Determinants of ultrafine particle exposures in transportation environments: findings of an 8-month survey conducted in Montréal, Canada. J. Expo. Sci. Environ. Epidemiol., 18, 551–563, https://doi.org/10.1038/sj.jes.7500644

Wiedensohler, A., Birmili, W., Nowak, A., Sonntag, A., Weinhold, K., Merkel, M., Wehner, B., Tuch, T., et al., 2012. Mobility particle size spectrometers: harmonization of technical standards and data structure to facilitate high quality long-term observations of atmospheric particle number size distributions. Atmos. Meas. Tech., 5, 3, 5, 657–685, https://doi.org/10.5194/amt-5-657-2012

Wiedensohler, A., Wiesner, A., Weinhold, K., Birmili, W., Herman, H., Merkel, M., Müller, T., Pfeifer, S., Schmidt A., Tuch, T., Velarde, F., Queincey, P., Seeger S., Nowak A., 2018. Mobility particle size spectrometers: Calibration procedures and measurement uncertainties. Aerosol Sci. Tech., 52, 142-164, https://doi.org/10.1080/02786826.2017.1387229

WHO, 2021a. Ambient (outdoor) air pollution. 22 September 2021, https://www.who.int/news-room/fact-sheets/detail/ambient-(outdoor)-air-quality-and-health

WHO, 2021b. WHO global air quality guidelines: particulate matter (PM2.5 and PM10), ozone, nitrogen dioxide, sulfur dioxide and carbon monoxide. World Health Organization. 273 pp, https://apps.who.int/iris/handle/10665/345329

WHO, 2013. Review of evidence on health aspects of air pollution – REVIHAAP Project Technical Report, https://doi.org/10.1007/BF00379640